NATIONAL AND KAPODISTRIAN UNIVERSITY
OF ATHENS
SCHOOL OF SCIENCE
FACULTY OF GEOLOGY AND ENVIRONMENT

MODELING COASTAL EROSION IN WESTERN PART OF NAXOS ISLAND

Maria Tzouxanioti

1114201300124

Supervisor: Prof. Niki Evelpidou

Athens 2021

Περίληψη

Σκοπός της παρούσας πτυχιακής εργασίας είναι η ταξινόμηση των ακτών της δυτικής Νάξου ως προς την τρωτότητά τους στην αναμενόμενη (μελλοντική) άνοδο της θαλάσσιας στάθμης εφαρμόζοντας τον Δείκτη Παράκτιας Τρωτότητας (ΔΠΤ) με τη χρήση Γεωγραφικών Συστημάτων Πληροφοριών (ΓΣΠ). Ο δείκτης αυτός επιτρέπει τη συνεκτίμηση έξι παραμέτρων με ημι-ποσοτικό τρόπο, με σκοπό την αναγνώριση περιοχών που είναι συγκριτικά περισσότερο ευάλωτες στις μεταβολές της θαλάσσιας στάθμης. Οι ημι-ποσοτικές παράμετροι είναι η παράκτια γεωμορφολογία, η παράκτια μορφολογική κλίση, ο ρυθμός μεταβολής της σχετικής στάθμης της θάλασσας, ο ρυθμός προέλασης ή υποχώρησης της ακτογραμμής, το μέσο εύρος παλίρροιας και το μέσο ύψος κύματος.

Η παράμετρος της γεωμορφολογίας σχετίζεται με την ανθεκτικότητα στη διάβρωση των παράκτιων γεωμορφών που οροθετήθηκαν με την χρήση διαφορικού DGPS-RTK Spectra Precision. Οι ρυθμοί προέλασης ή υποχώρησης της ακτογραμμής προέκυψαν από επιτόπια έρευνα και μελέτη τοπογραφικών διαγραμμάτων. Η μορφολογική κλίση υπολογίστηκε χρησιμοποιώντας το Ψηφιακό Μοντέλο Εδάφους. Για τις υπόλοιπες παραμέτρους χρησιμοποιήθηκαν βιβλιογραφικά δεδομένα.

Η ακτογραμμή της περιοχής μελέτης διαιρέθηκε σε τμήματα μήκους 20 m και για κάθε τμήμα εκτιμήθηκε η τιμή του Δείκτη Παράκτιας Τρωτότητας ως η τετραγωνική ρίζα του γινομένου των τιμών των έξι μεταβλητών προς τον αριθμό 6 που είναι το σύνολο των παραμέτρων που ελήφθησαν υπόψη.

Οι τιμές του δείκτη που εκτιμήθηκαν για την περιοχή κυμαίνονται από 5.0 έως 32.0 με τις περισσότερο τρωτές περιοχές (πολύ υψηλή και υψηλή τρωτότητα) να εντοπίζονται στην περιοχή του Αγίου Γεωργίου, Αγίου Προκοπίου, Αγίας Άννας, Πλάκα, Μικρή Βίγλα, Καστράκι, Πυργάκη και Αγιασσός. Αντίθετα, συμπεραίνεται ότι οι ακτές που καταλαμβάνονται από παράκτιους βραχώδεις κρημνούς, είναι λιγότερο ευάλωτες χωρίς κάποια εξαίρεση.

Λέξεις κλειδιά: Δείκτης Παράκτιας Τρωτότητας, Παράκτια Γεωμορφολογία, Διάβρωση, Προέλαση, Ακτογραμμή, Νάξος, Κυκλάδες, Μεταβολή Θαλάσσιας Στάθμης, Γεωμορφές

Abstract

This thesis is specifically concerned with the classification of the coast of the western Naxos Island according to its vulnerability to an anticipated future sea-level rise, using the Coastal Vulnerability Index (CVI) and utilizing Geographic Information Systems (GIS) technology. This index relates in a semi-quantitative manner the following six physical variables, geomorphology, coastal slope, relative sea-level rise rate, shoreline erosion or accretion rate, mean tidal range and mean wave height, aiming to identify areas that are comparatively more vulnerable to sea level change.

The variable of geomorphology expresses the relative erodibility of various coastal landforms and was derived from detailed field geomorphological mapping. Shoreline erosion or accretion rates were obtained from interpretation of field survey and topographic maps. The slope of the coastal zone was estimated using the Digital Elevation Model (DEM) of the area derived from topographic maps at the scale of 1:5,000. Bibliographic data were used for the mean tidal range, mean wave height and relative sea level change

The shoreline of the study area was divided into sections, with a length of 20.0 m. The Coastal Vulnerability Index (CVI) was estimated for each section, as the square root of the values of the ranked variables divided by their total number involved.

According to the produced CVI values (ranking between 5.0 and 32.0), the most vulnerable coastal regions (of high and very high vulnerability) were found along the coastal area of Agios Georgios, Agios Prokopios, Agia Anna, Plaka, Mikri Vigla, Kastraki, Pirgaki and Agiassos. However, it was concluded that steepy rocky coast areas are the least vulnerable sections of understudy shoreline.

Key words: Coastal Vulnerability Inditex, Coastal Geomorphology, Erosion, Accretion, Coastline, Naxos Island, Cyclades, Sea Level Rise, Landforms

Acknowledgments

After the completion of the present dissertation my studies in the undergraduate program of the Department of Geology and Geoenvironment of the University of Athens are completed.

This dissertation would not have been possible without the encouragement of many individuals. At this point I would like to extend my deepest gratitude to my supervisor, **Professor Niki-Nikoletta Evelpidou**, for the assignment of the subject, for the trust towards me and her valuable guidance.

I would like to recognize the invaluable assistance of **Msc. Apostolia Komi** and **Msc. Aikaterini Giannikopoulou** for their support in methodology and ArcGIS.

Last but not least, I would like to express my gratitude towards my family and friends who were always by my side and for their encouragement which helped me to pursue and fulfill my undergraduate studies.

Table of contents

1. Introduction

The coastal zone is a natural system that is directly affected by the interaction between the lithosphere, the hydrosphere, and the atmosphere, as well as by the action of terrestrial, aerial, and marine processes. It is an environment which constantly changes over time through slow-moving phenomena, the duration of which may vary from as long as a thousand years to a rapid action within even twenty-four hours. Apart from its unique physical characteristics, the coastal zone is also of great interest for the plethora of resources it offers.

About 41.0% of Europe's population lives near the coast, leading to increasing urbanization rates (Collet & Engelbert, 2013). The coastal zone hosts a number of tourism businesses and activities, making, therefore, the tourism industry one of the most important sectors of the economy at local and national level. Among the various types of coasts, sandy coasts are more encumbered by this type of activity (Davenport & Davenport, 2006) and they are among the most geomorphologically complex coasts, with the coastline constantly changing under the interaction between natural and anthropogenic factors (Mentaschi *et al*., 2018; Vousdoukas *et al*., 2020).

Apart from the natural factors that contribute to the evolution of the coastal zone such as eustatism, tectonics and more, the climate change in recent decades is capable of causing significant changes in coastal areas, mainly due to rising sea levels, with the coastline being the main receiver of these changes. Coastal environments are in a dynamic interaction with marine processes where coastal sediments are constantly moving, either resulting in the formation of a new coastline or the erosion of an existing coastline. The phenomenon of erosion is intensified by rising sea levels, as well as by anthropogenic interventions, thus increasing the vulnerability of the coastal zone (Briguglio, 2004).

According to Vousdoukas *et al*., (2020), 13.6–15.2% (36,097–40,511 km) of sandy coasts worldwide could be severely eroded by 2050, with these figures rising to a percentage of 35.7%-49.5% (95,061–131,745 km) by the end of the century. In the case of Greece, the coastline reaches 18,400 km for the mainland and 9,835 km for the islands (Poulos & Chronis, 1997).

Erosion along the coasts is estimated at 6.1% for Thrace and Eastern Macedonia, 10.3% for Central Macedonia, 2.3% for Thessaly, 14.7% for the North

Aegean islands, 25.9% for the Cyclades and the Dodecanese, 3.8% for the Peloponnese and 6.1% for the coasts of Northern Crete (Alexandrakis *et al*., 2010). In the Cyclades and Dodecanese region, 51.0% of the coastline consists of low escarpments with slopes of 6.0-9.0% and 46.0% of pocket beaches of low slopes (Alexandrakis *et al*., 2010).

Since the end of the 19th century, global sea levels have risen by about 1.6 mm/year (Church and White, 2011), while its rate has not exceeded 0.6 mm/year over the past two millennia (Kemp *et al*., 2011). In time scales ranging from decades to centuries, sea levels vary, mainly due to anthropogenic climate change and its effects on the melting of glaciers and ice caps and the thermal expansion of the oceans (Milne *et al*., 2009; Church *et al*., 2011). As sea levels are expected to rise further in the future (0.5 to 1.0 m by 2100 and possibly more, Church *et al*., 2013), concerns about its future impact on coastal areas are also increasing (Hinkel *et al*., 2012; Hallegatte *et al*., 2013; Mimura, 2013).

According to a recent report by the Intergovernmental Panel on Climate Change (IPCC, 2019), the predominant sources of freshwater supply leading to global Mean Sea Level (GMSL) are glaciers and ice caps. From tide gauge observations and satellite altimeter observations, GMSL has increased from 1.4 mm/year in the period 1901-1990, to 2.1 mm/year in the period 1970-2005, to 3.2 mm/year in the period 1993-2015 and to 3.6 mm/year in the period 2006-2015. GMSL in 2019 was the highest ever measured. Representation of GMSL based on tidal observations shows an increase of 19.0 cm from 1900 until today (Dangendorf *et al*., 2019).

Estimates of projected future changes in this report are largely based on the predictions of the CMIP5 climate model using Representative Concentration Pathways (RCPs). RCPs are scenarios that include time series of emissions and concentrations of the full range of greenhouse gases (GHGs), aerosols and chemically active gases, as well as land use / land cover. RCPs provide only a set of many possible scenarios that would lead to different levels of global warming. The future increase of GMSL caused by thermal expansion, melting of glaciers and ice caps and changes in water storage, largely depends on which scenario is followed. At the end of the century, sea level rise is expected to be faster in all scenarios, including those that are compatible with achieving the long-term temperature target set by the Paris Agreement (Oppenheimer *et al*., 2019).

2. Study area

2.1. General information

Naxos is the largest island (429.79 km^2) in the Cyclades, with a coastline that reaches 148.00 km and the highest altitude of ~1004.0 m (mountain Zeus). It is located in the center of the Aegean Sea and at a short distance from Paros (east) (Figure 1). In the south-southeast of Naxos there are the islands Iraklia, Schinoussa, Koufonisi, Kato Koufonisi, Keros and Ano and Kato Antikeri. To the east there the islets of Makares, Agia Paraskevi, Stroggyli and Donousa are located.

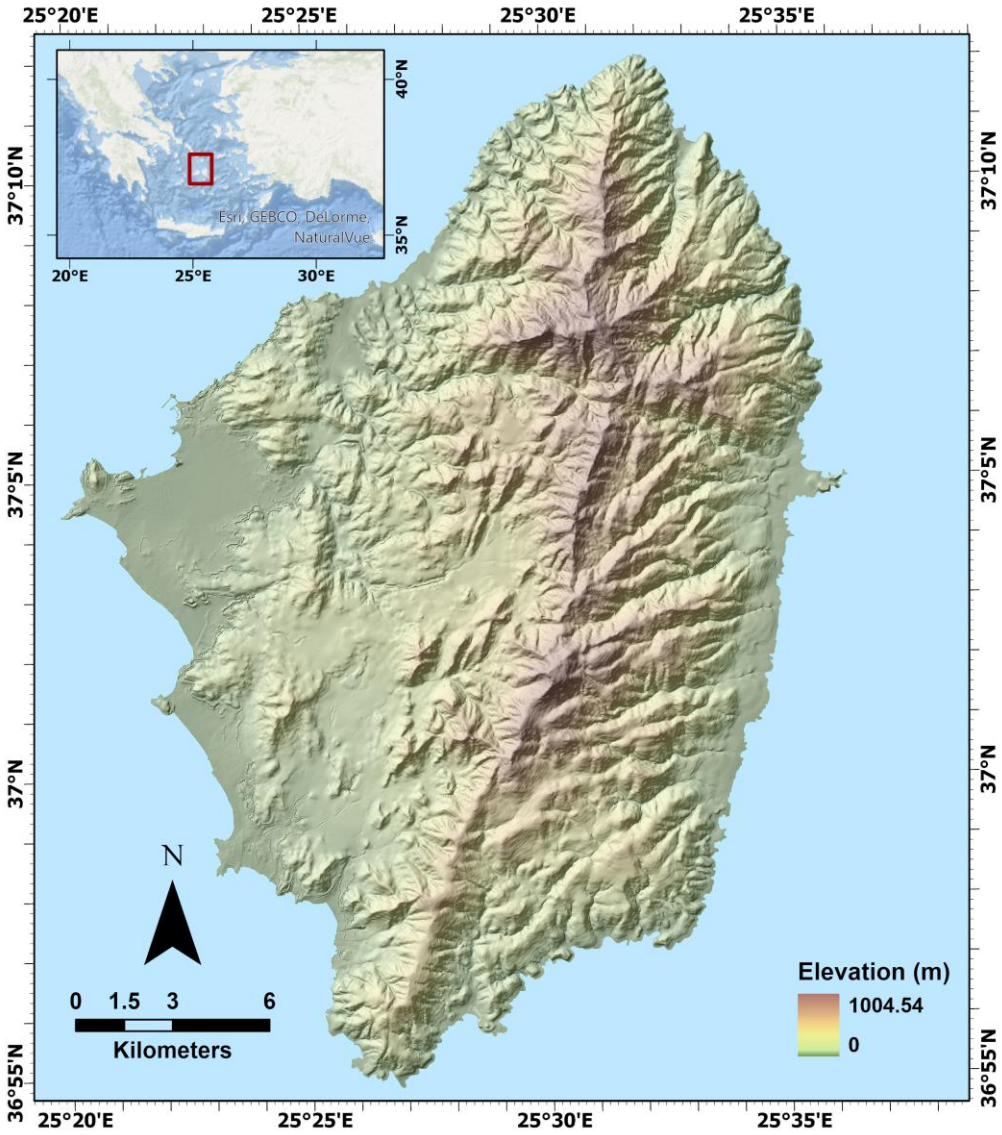

Figure 1: Naxos Island, located at the center of the Cyclades islands, Aegean Sea.

The relief is mountainous, with a central mountain range that crosses the island from its north to the southern end. The maximum altitude of the area is ~1004.0 m at the top of Mount Zeus, which is approximately in the center of the mountain range.

The shape is elongated, with a maximum axis of 32.77 km and a minimum of 23.86 km. From the northern part of the island and towards its southwestern coasts, there is a division with the bays of Limenari Kyra, Amyti, Agios Georgios and Kyrades where the islands of Amaranthos, Aspronissi, and Virgo are located. Still, there is the cape of Kavos, Mikri Vigla, Kouroupia, and Katomeri. The eastern coastline has a significant division, except for Asala Cave and Cavo Stavros, compared to the west coast.

According to the Kallikratis program (law 3852/2010) in Greece, it belongs to the Region of South Aegean, to the Regional Unity of the Cyclades and together with the Small Cyclades (Iraklia, Schinoussa, Koufonissi, Donousa) constitutes a single Municipality of Naxos and Small Cyclades consisting of 4 Municipal Communities and 18 Municipal Districts. According to the latest census of 2011, its population is 1,793,000 inhabitants.

2.2. Climate

2.2.1. Rainfall

Naxos has an extremely low rainfall (Theocharatos, 1978). On December and January, the highest rainfall is expected to be of 68.70 mm and 67.60 mm, respectively (HNMS 1955-1977). The average annual rainfall is 366.80 mm, but since the meteorological station is in Naxos, it is expected to be slightly higher on Zeus Mountain.

2.2.2. Temperature

Winter is particularly mild in the Cyclades. In the mountainous regions of Naxos, temperatures are lower by 2-3^{o}C. In summer, temperatures are lower than the majority of other Greek regions and always remain below 26°C (HNMS, 1955-1977). This is due to the effect of the sea, but also to the winds with high frequency and intensity, resulting in a decrease of temperature. During the summer months evaporation is particularly noticeable. This happens due to increased temperature, low humidity in the air, moderate soil humidity, high sunshine, and strong winds.

The average annual temperature is 18.18°C (HNMS, 1955-1977) and the annual temperature range is 12.7°C (HNMS, 1955-1977). The warmest month is July with a mean highest temperature of 26.8°C and the coldest is February with a mean lowest temperature of 9.3°C (HNMS, 1955-1977).

2.2.3. Wind

The prevailing wind direction throughout the year is from north to south. Moreover, the climate of the island and the central Aegean as well, is generally characterized by the annual winds that blow from northern directions, during the summer period. The intensity of the winds takes its highest value in the early afternoon hours and can reach zero level during the night. Their formation is due to the presence of an extensive barometric low that is usually found in the summer in northwest India.

2.2.4. Humidity

As calculated, within the period 1955-1977, the average annual humidity value of Naxos is 72.00%. The wet months are November, December, and January with small differences, while the difference between the driest and the wettest month does not exceed 5.80%.

2.3. Hydrographic network

In the islands of the Cyclades, the existence of karst aquifers of limited area that are developed in carbonate formations is typical. The hydrographic network of Naxos has dendritic form (Figure 2). Most of the rivers and torrents of Naxos originate from the mountainous part of the island and flow perpendicular to the coastline. The largest branch of the hydrographic network is of 4th (IV) Strahler order (Strahler, 1957) (Figure 2).

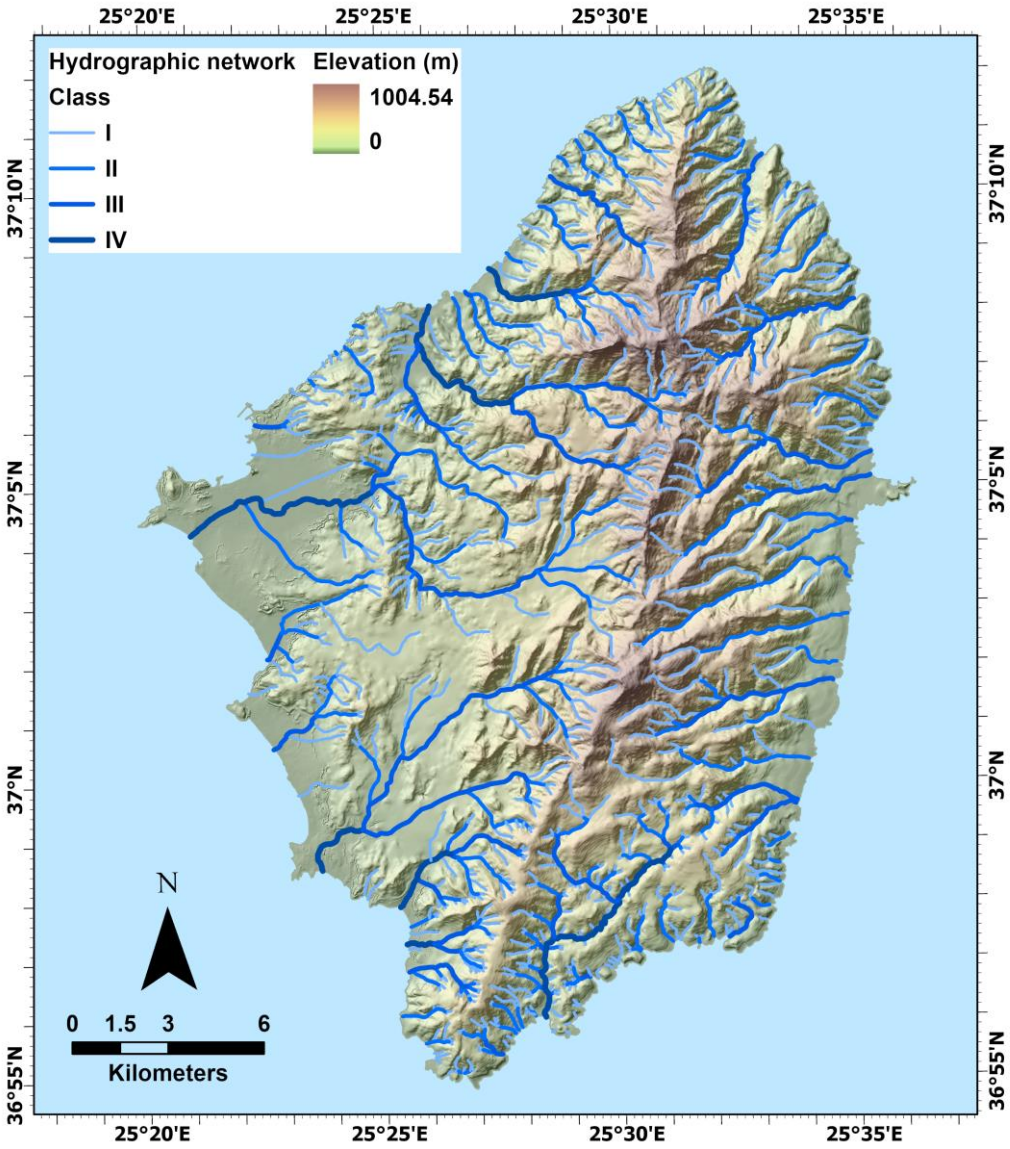

Figure 2: Hydrographic network of Naxos Island.

2.4. Land uses

The land uses of the island of Naxos have been recorded using data from the CORINE 2018 database (Figure 3). In fact, the largest area of the island is covered by forest and seminatural areas with a percentage of 63.07% (Table 1). The category named forest and seminatural areas includes natural grassland areas, sclerophyllous vegetation, transitional woodland/shrub, beaches, dunes, and sand plains and sparsely vegetated areas. The agricultural areas occupy a smaller area with a percentage of 35.16% (Table 1). Agricultural areas include rice fields, olive groves, pastures, meadows and other permanent grasslands under agricultural use, complex cultivation patterns and land principally occupied by agriculture, with significant areas of natural

vegetation. Even smaller area is occupied by artificial surfaces with percentage of 1.33%, wetlands with percentage of 0.06% and water bodies with percentage of 0.38% (Table 1).

Type of land use	Area (km^2)	%
Artificial surfaces	5.74	1.33
Agricultural areas	150.92	35.16
Forest and seminatural areas	270.72	63.07
Wetlands	0.27	0.06
Water bodies	1.62	0.38

Table 1: Extent and percentage of land use coverage.

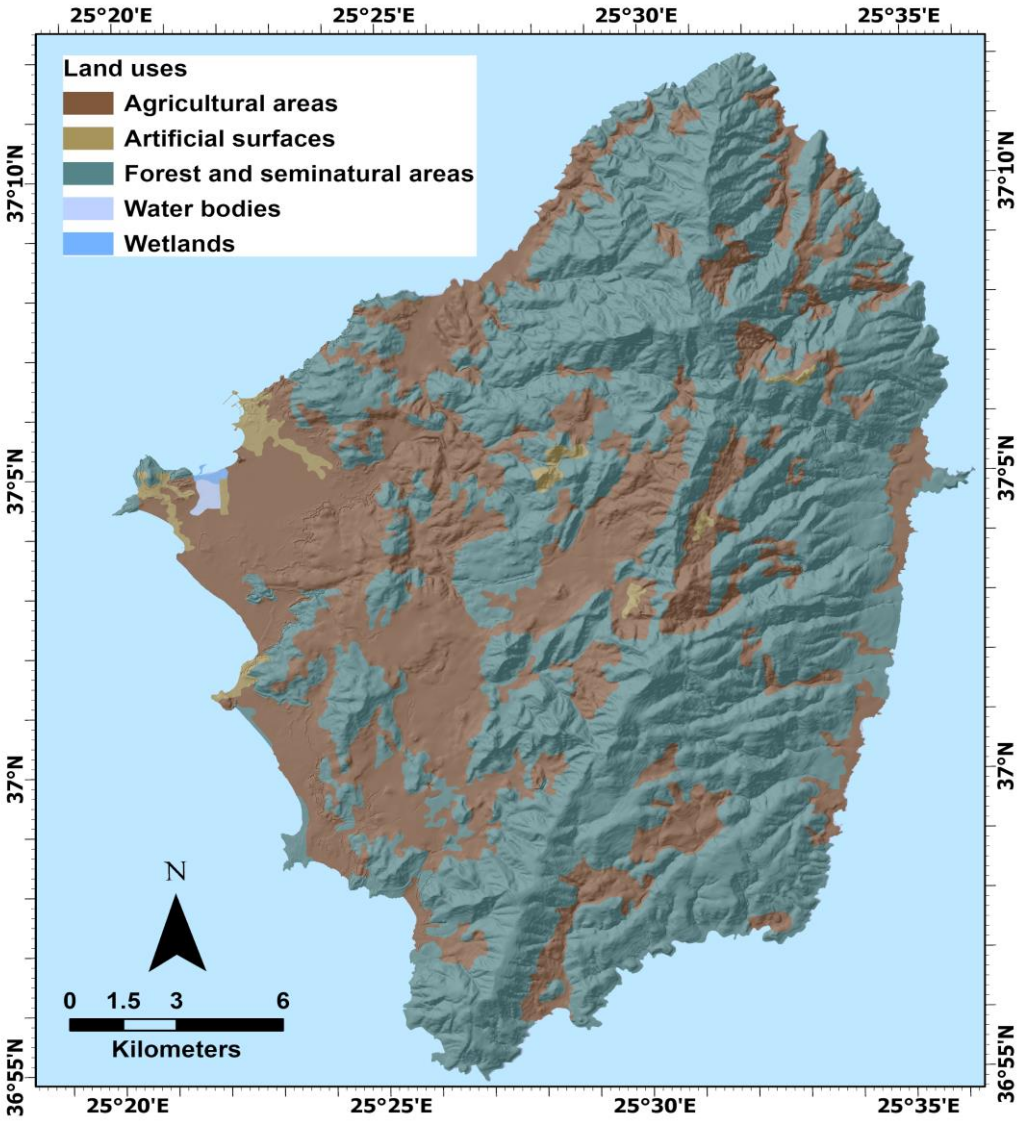

Figure 3: Naxos Island land uses coverage map according to CORINE 2018.

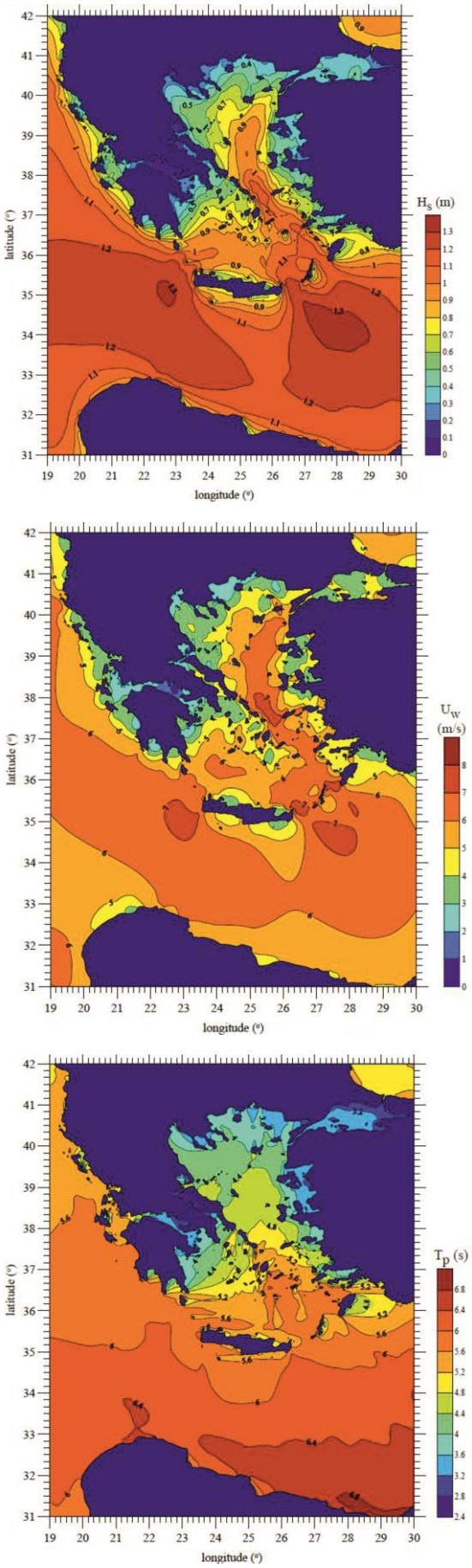

2.5. Oceanographic data

According to the "Atlas of Wind and Wave of the Greek Seas" (Soukissian *et al*., 2007), the western area of Naxos is characterized by an annual average significant wave height (Hs) of 0.7-0.8 m (Figure 4a), annual mean wind speed (Uw) 5-6 m/sec (Figure 4b) and annual average wave period (Tp) 4.8-5.2 sec (Figure 4c).

Figure 4: (a) Spatial distribution of mean value of annual significant wave height (Soukissian et al., 2007). (b) Spatial distribution of mean value of annual mean wind speed (Soukissian et al., 2007). (c) Spatial distribution of mean value of annual mean wave period (Soukissian et al., 2007).

3. Geological setting of Cyclades

The Cyclades are part of the Hellenides (Kober, 1928). The Cyclades are made up of several tectonic thrust units, consisting of the Pelagonian, Pindos, Gavrovo-Tripolitza, Phyllite-Quartzite, and Ionian (van Hinsbergen *et al*., 2005).

The dominant sequence is the Cycladic Blueschist unit, which is considered to be a paleogeographic equivalent of the Pindos unit (Bonneau, 1982). This consists of a polymetamorphic Carboniferous Permian to the latest Cretaceous passive margin sequence that tectonically overlies the Cycladic Basement unit (Blake *et al*., 1981). Some tectonic windows of the Cyclades (basal unit) depict a trace of a Late Triassic to Late Cretaceous carbonate platform (Avigad & Garfunkel, 1989) and are exposed below the Cycladic Blueschist unit.

The Basal unit shows evidence of high pressure-low temperature metamorphism (Shaked *et al*., 2000). The Basal unit is considered to be part of the External Hellenides (Avigad *et al*., 1997). The rocks of the Cycladic Blueschist unit were exhumed in two successive stages corresponding to two metamorphic episodes (Jolivet & Brun, 2010), with the first stage occurring during Eocene Hellenic subduction, exhuming Blueschist and eclogite faces assemblages (Altherr *et al*., 1979; Wijbrans & McDougall, 1988; Wijbrans *et al*., 1990), likely in an extrusion wedge (Ring *et al*., 2007, 2010; Huet *et al*., 2011).

During subsequent tectonism in the Oligocene and Miocene, exhumation occurred as Cordilleran type metamorphic core complexes (Lister *et al*., 1984) with mainly NE-dipping low-angle normal faults ("detachments") showing a dominant top to the N or NE sense of shear (Buick, 1991; Gautier *et al*., 1993; Vanderhaeghe, 2004).

These rocks part of the Pelagonian unit, consist of a Paleozoic basement with a Paleozoic and Mesozoic carbonate cover overlain by a Jurassic ophiolite (Bonneau, 1982), and they have locally endured a Late Cretaceous high-temperature metamorphic event (Reinecke *et al*., 1982; Altherr *et al*., 1994; Zeffren *et al*., 2005).

4. Geological setting of Naxos Island

The dominant part of Naxos comprises a sequence of deformed and metamorphosed Mesozoic platform sediments (marbles with dolomite, metapelites, and metapsamites) that surround a deeply eroded NNE (N15^{o}E) structural migmatite dome in the central part of Naxos (Figure 5).

Its migmatite core consists of orthogneises, containing marble and metapelites. The core is covered by schists such as metapelites containing horizons of ultramafic lenses, amphibolites, and gneiss, with an age of 515 MA as measured by isotope Rb/Sr. In the upper part of the structure, we find metaconglomerate and emery deposits. The migmatite dome is a pre alpine background. As a result of isoclinal folds (with Eocene age), metapelites and marbles have been identified in alternations (Andriessen *et al*., 1979; Durr, 1986).

In the west of Naxos there is an extensive outcrop of type I granodiorite. The age of granodiorite's intrusion has been defined at 25±5 MA after radiocarbon dating and the age of sterilized is at 10 MA.

Both the metamorphic complex and the granodiorite are overlain by fault bounded slices of sediments, the allochthonous unit, in which, a number of types of non-metamorphic igneous rocks occur (Figure 5). S Type granites are mainly found in the northern part of the island like aplite and pegmatite dikes, relatively undeformed. In the western part of Naxos Island, Neogene and Quaternary sediments are found.

Thus, Naxos Island is an elliptic dome. In its center, there are migmatites while in the circumference schists, marbles and gneiss are appeared with lots of folds and in alternation. More specifically, schists, marbles, and gneiss cover 76.96% of the mainland (Figure 5). Granodiorite covers the 8.42%, migmatite the 7.14% and the sedimentary rocks the 7.47% (Figure 5).

4.1. Metamorphism

Metamorphism is described into seven metamorphic zones with temperatures from 330^{o}C till 720^{o}C and above (Wijbrans & McDougall, 1986). These isograds increasing in grade towards a core of migmatite have been mapped by Jansen and Schuiling (1976): zone I (diaspore), zone II (chlorite-sericite), zone III (biotite-

chloritoid), zone IV (kyanite), zone V (kyanite-sillimanite and sillimanite), zone VI (migmatite) (Table 2, Figure 5).

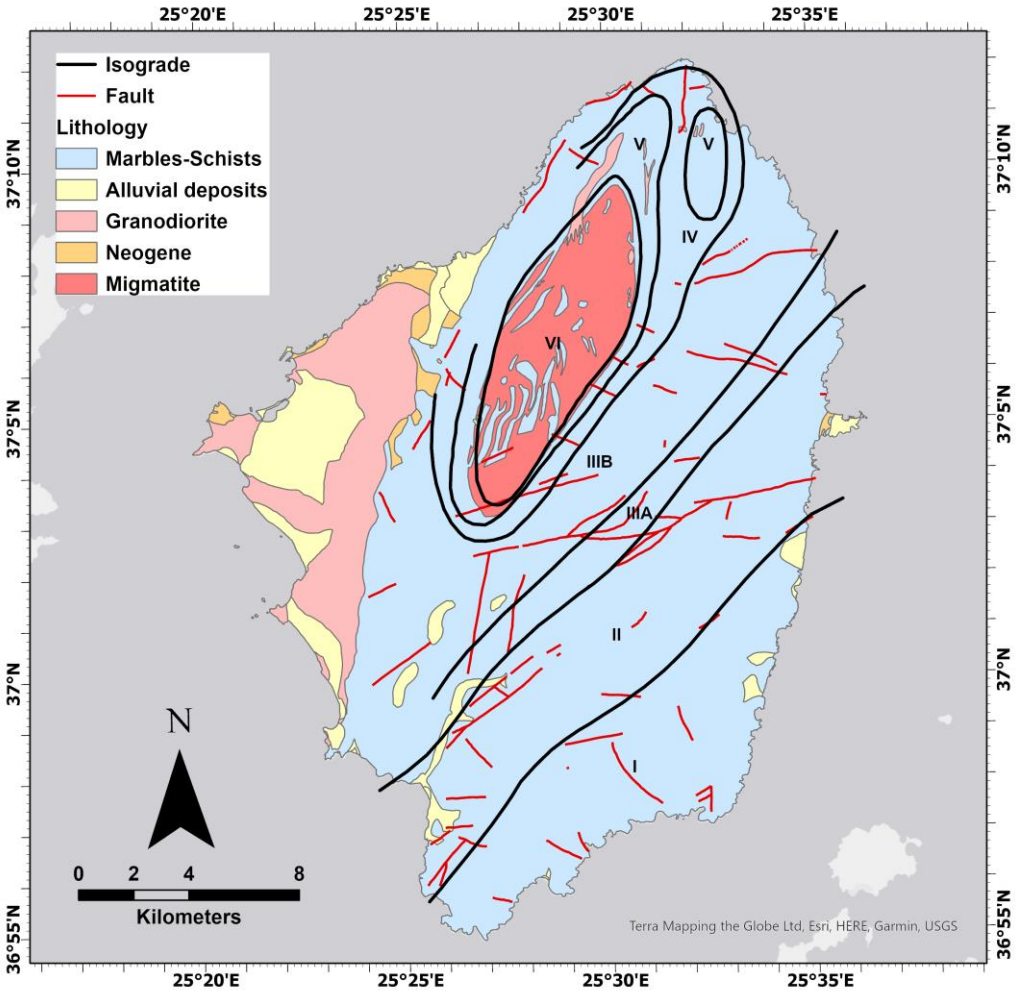

Figure 5: Simplified lithological map of Naxos with main faults and metamorphic zones.

Metamorphic zone		Temperature (°C)
I	Diaspore zone	380
II	Chlorite-sericite zone	440-420
III	Biotite-chloritoid zone	~500
IV	Kyanite zone	560-540
V	Kyanite-sillimanite zone	~620
	Sillimanite zone	~650
VI	Migmatite zone	690-660

Anatexis zone	~700

Table 2: Metamorphic zones and their related temperature according Jansen and Schuiling (1976).

The age of each metamorphic series occurs from marbles. The area Za is located northeast, in which not only algae and foraminifera of the upper Triassic (Durr & Fluegel, 1979) where found but also a significantly metamorphic series of dolomitic, calcite marble with fossils giving Mesozoic ages with a probability of existence and Paleozoic segment at the base of the series (Jansen 1977; Durr 1986). Furthermore, within the marbles, there is emery which corresponds to second bauxite horizon of Central Greece with an age of upper Jurassic (Feenstra, 1985).

According to Durr (1986), the marbles entail hornfels of Jurassic age. In the island of Naxos, the metamorphic phenomena and the metamorphic zones as well are due to a strong reheat (higher point before the 25 MA.), with the mantle as a source and means of heat transfer a fluid phase of CO_2. At the end of reheating, we have anatexis of many rocks (metamorphic zone VI) and granite intrusion as well in the north and northwest section of the island. Metamorphic phase sequence in Naxos according to Andriessen *et al*. (1979):

- upper Eocene (45±5 MA) Blueschist phase with pressure above 10 kbars and temperature at 450-480^{o}C (HP/LT),
- Oligocene-upper Miocene (25±5 MA) reverse greenschist phase with pressure 5-7 kbars and temperature at 500-700^{o}C (LP/HT),
- in the next metamorphic phase with age 111±0,7 MA we have a rise of granodiorite, and
- the last metamorphic phase with age 10 MA is connected to the youngest Alpine thrusts.

Above the metamorphic series, there are remains of non-metamorphic rocks which are sections of the Pelagonian nappe, ophiolite nappe of Greece and the Mesohellenic molasse (Durr, 1986).

4.2. Deformation

4.2.1. Brittle deformation

Naxos faults can be classified as:

- low angle normal faults, along which the emplacement of the allochthonous tectono-sedimentary unit over the granodiorite and the metamorphic complex,
- normal faults with a strike-slip component, trending EW, related to the final stages of the migmatite core uplift, and
- normal faults of the Pliocene and Quaternary ages of various trends.

4.2.2. Ductile deformation

4.2.2.1. Folds

From Eocene till today, three generations of folding have been identified on Naxos Island:

- first generation (F1) isoclinal, developed prior to the peak of reverse greenschist,
- second generation (F2) tight to isoclinal northwards trending asymmetric folds to the peak of reverse greenschist, and
- third generation (F3) upright NS trending usually open folds formed after the peak of reverse.

4.2.2.2. Shear zones

Two major ductile shear zones have been recognized on Naxos Island:

- one, NNE trending associated with an extension that has been affected by the third generation folding, and
- a second shear zone has been identified at the contact of granodiorite and metamorphic complex.

4.2.2.3. Naxos dome

The Naxos dome was originally described as a static thermal overprint on an earlier anticline structure, formed during the peak of reverse greenschist metamorphic phase (M2) deformation. The parameters P (pressure) and T (temperature) obtained for M2 though imply a temperature rise while important decompression took place. This leads to the deduction that the dome is structural in its origin.

5. Geomorphological setting of W. Naxos Island

Erosional processes and tectonic forces are the major factors in the formation of the landscapes and landforms of the area. According to Evelpidou (2001), the lithology of Naxos is consisted of various lithological formations with different resistance in erosion, which, in combination with the action of the hydrographic network and tectonics, has created the present morphology. The erosion in Naxos mainly occurs through runoff erosion, which, in combination with the transported material, pre-existing discontinuities get extended, creating a variety of geomorphological landscapes. One of the main processes sculpting the landscape of Cyclades and Naxos is the differential erosion, due to variations in vulnerability of the geological formations. Depositional processes have contributed to the present-day landscape at the western part of the island.

In the coastal zone, the most characteristic landforms are owed to depositional processes with notable examples of coastal dunes, lagoons, tombolos, as well as beachrocks mainly located on the west coast while erosional processes have formed tafoni, marine notches (Evelpidou *et al*., 2014), coastal cliffs (Figure 6).

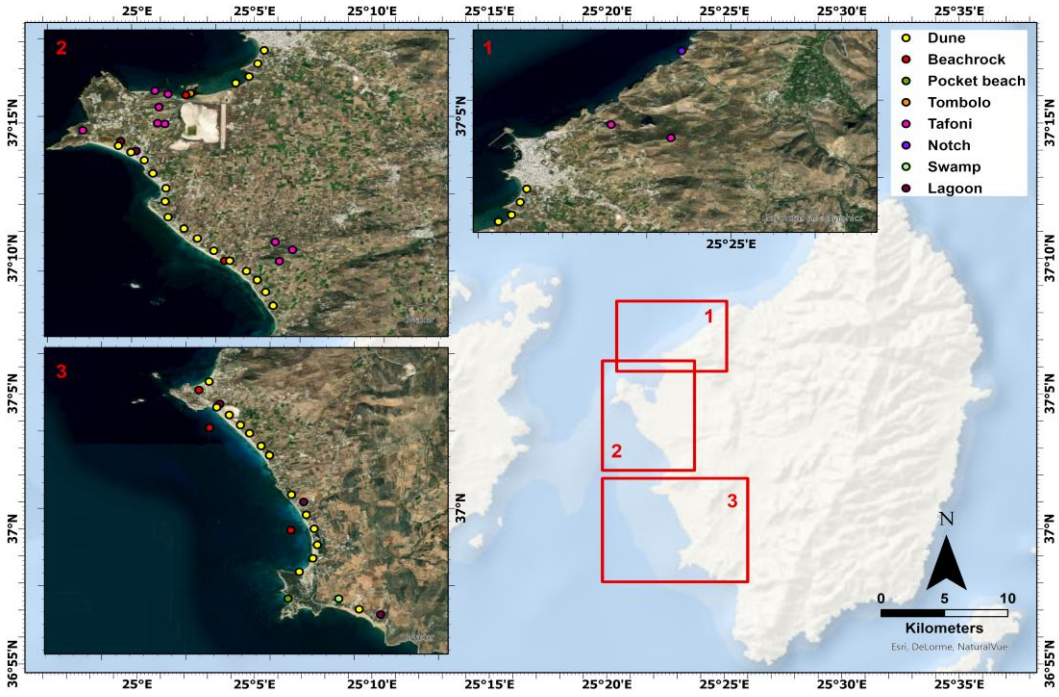

Figure 6: The western part of the island is characterized by the presence of coastal dunes, lagoons, tombolos, beachrocks, tafoni, notches, coastal cliffs, and pocket beaches.

The biological erosion processes have created landforms called tidal notches, which are located in the submarine part of Naxos coast.

5.1. Tafoni

Tafoni are cavernous, cellular geomorphological formations of weathering which typically are several cubic meters in volume and have ellipsoid or spherically rotating, extending internally to the aperture shape, concave inner walls, overhanging margins (visors) and smooth gently sloping, debris covered floors (Mellor *et al*., 1997). They occur mainly in crystalline rocks of medium to large granules, but also in other types of rocks, such as sandstones, limestones and shales in many parts of the world (Goudie & Viles, 1997; Goudie *et al*., 1997), including polar regions. The largest tafoni often appear by thin walls, have a vaulted shape and their opening is in the lower part and has a smoother shape. Their origin is related to the action of the wind and, especially, water.

At Naxos Island, tafoni appear mainly in its western part, formed in the granodiorite of Stelida (Figure 7). In recent research (Evelpidou *et al*., 2021), about 200 tafoni have been extensively studied for their geomorphological characteristics, mineralogy, and geochemistry. Their dimensions vary from a few centimeters to a few meters. The increased presence of mica and gypsum, as well as the presence of alite, suggests that disintegration due to salts (moisture and seawater spray) plays an essential role in their development (Evelpidou *et al*., 2021).

Figure 7: Tafoni formation in Stellida area. Tafoni also divided into compartments by remnants of vertical walls.

5.2. Sand dunes

The term coastal sand dunes refers to the geomorphology created by the combined action of aeolian transports of sand and an obstacle wind flow (e.g vegetation, dry branches, depressions, protrusions, etc.). The morphological characteristics of the dunes, in general, are related to the amount of sand that can be transported by the wind and the deposition-erosion cycles. The dimensions of the sand dunes vary, and their diameters range from a few meters to several kilometers. Their height ranges from 1 m or 2.0 m up to 20.0-30.0 m.

Sand dunes are formed in any environment, where loose pieces of rock, the size of a grain of sand, are exposed to the action of the wind and can easily migrate and accumulate in non-compact masses. Every accumulation of soil, protrusion or depression, the presence of vegetation, etc. also contributes to this accumulation. Also, the presence of moisture can stabilize the concentration of sand, which will eventually be the beginning of a dune formation.

Dunes are found mainly along the west coast. However, dunes have also been found on the east coast. On the west coast they extend almost continuously from Chora to Pyrgaki, 20.0 km to the south in Agios Georgios, Agia Anna, Plaka (Figure 8), Kastraki, Glyfada (Figure 9) and Pyrgaki.

Figure 8: Aerial photo of Plaka area.

Figure 9: Aerial photo of Glyfada area.

5.3. Tombolo

It is a geomorphic feature formed when a crescent-shaped shore connects the coastline with an island adjacent to the shore, rocky or sandy. The term tombolo originated from Italy and referred to one or more sandy isthmus-shaped formations that were connected to the land. This is a fairly common landform along closed coastlines, which are in the youth stage or at the beginning of the maturity stage. In the areas where a double Tombolo is formed, a lagoon is created between the two landforms, which is gradually filled with tilted material and thus a wide flat ridge is formed (Figure 10).

Figure 10: Panoramic view of Agios Georgios area. At the west coast of Naxos there is a characteristic Tombolo, in the area laguna of the airport. Its development is owed to coastal currents that transported and deposited the sand between Manto island and the adjacent beach.

5.4. Beachrocks

Beachrock was first defined by Scoffin and Stoddart (1987) as "the consolidated deposit that results from lithification by calcium carbonate of sediment in the intertidal and spray zones of mainly tropical coasts". Beachrocks can record the vertical and the horizontal evolution of the shoreline in a paleo-environment. The primary mechanisms proposed for the origin of beachrock cements as follows:

- physicochemical precipitation of high Mg calcite and aragonite from seawater (result of high temperatures, $CaCO_3$ super saturation, and/or evaporation (Ginsburg, 1953; Stoddart & Cann, 1965),
- physicochemical precipitation of low Mg calcite and aragonite by mixing of meteoric and fresh groundwater with seawater (Schmalz, 1971),
- physicochemical precipitation of high Mg calcite and aragonite by degassing of CO_2 from beach sediment pore water (Thorstensen *et al*., 1972; Hanor, 1978), and
- precipitation of micritic calcium carbonate as a byproduct of microbiological activity (Taylor & Illing, 1969; Krumbein, 1979; Strasser *et al*., 1989; Molenaar & Venmans, 1993; Bernier *et al*., 1997).

In the coastal and underwater area of Agios Georgios in Naxos, 3-4 rows of beachrocks are developed that extend from the sea level up to a depth of 6.2 m (Karkani, 2017; Karkani *et al*., 2017) (Figure 11), in contrast to the area of Plaka where at least 3 rows are developed, reaching a length of more than 2.5 km and a depth of 6.2 m (Karkani, 2017; Karkani *et al*., 2017) (Figure 12).

Figure 11: Beachrocks in Agios Georgios area.

Figure 12: In the south part of Plaka, submerged beachrocks are almost parallel to the modern coastline. Beachrocks usually develop in bands, parallel to the beach. They may extend along a long stretch of coast, but they are also found in patches, covering only part of the coast.

5.5. Lagoons

The term lagoon is used to define a water basin, which extends parallel to the coastline and is separated from the open sea by barrier island. It is usually developed diagonally towards the estuary of one or more torrents and therefore the calm waters behind the island dam are an ideal environment for the deposition of torrent materials. Lagoons are usually shallower than river bays, making their bottom more vulnerable to wave action. The turbulence caused by the waves can lift the tilted sediment of the seabed, as well as the torrent material, so that the finer material is transported to the sea through the passages between the island dams. In the western part of the island lagoons are located in the area of Agios Georgios, Agios Prokopios, Mikri Vigla (Figure 13) and Glyfada.

Figure 13: Lagoons at Mikri Vigla beach. Lagoons are usually shallower than rivers, so their bottom is prone to wave action. Infront of them sand dune fields are usually developed.

5.6. Cliffs

Coastal cliffs are steep coastal slopes which result from the action of marine processes. In environments where the wave action is predominant, these slopes have a large morphological slope or can be vertical surfaces. The role of wave erosion is twofold, as it not only corrodes the base of the cliff front, but it also removes the products of disintegration from its base. When the products of disintegration accumulate at the base of the cliff front, it is possible to slow down or stop its retreat, as they protect the cliff front from the waves that crash into it. The resistance of the cliffs to corrosion depends on the wave energy and the cohesion of the rocks of which the slopes are composed. A typical example of a coastal cliff is Hawaii beach (pocket beach), located in the SW part of Naxos (Figure 14).

Figure 14: A typical example of a pocket beach is Alyko (Hawaii) Beach, located in the SW part of Naxos. The erosion material of the cliff produces the wide and long beach in front of it.

5.7. Notches

Marine notches are recesses along coastal cliffs. They are found in those places where the sea meets the land and due to processes of friction, dissolution, or biological factors, these forms are created. The appearance of coastal notches above sea level indicates tectonically active areas. Depending on their origin and form, they are classified into dissolution notches, structural notches, lithological notches, wave erosion notches, sub-tidal (or sublittoral/infralittoral), supralittoral, and midlittoral notches (Pirazzoli, 1986). Tidal notches stand out among geomorphological indicators, as they can indicate old sea levels with an accuracy of one centimeter, while their morphology provides qualitative information about sea level change rates and tectonic movements (Evelpidou & Pirazzoli, 2014).

Evelpidou *et al*., (2014), combining the morphology of submerged notches in Naxos, the history of seismicity in the area and correlating their findings with archaeological information, they found that rapid subsidence events took place, with possible seismic origin. These relative changes in sea level date back to 3,300 years ago. From the analysis of the tidal notches in Naxos, the average sinking rate was estimated between 0.3 mm and 1.54 mm/year. Associating the submerged paleoshoreline at -2.8 m with archaeological information from Grotta. Evelpidou *et al*. (2014), dated this deepest notch to 3,300 years ago, thus estimating more accurately the sinking rate for the last 3 millennia, at 0.8-0.9 mm/year. In addition, the presence of the shallowest paleoshoreline at depths of 30.0-40.0 cm, both in Naxos and other Cycladic islands (Sifnos, Antiparos, Paros, Heraklia, Keros), showed a recent sinking, which is due to the recent sea level rise in the last two centuries, but also in the earthquake of Amorgos in 1956 (Evelpidou *et al*., 2012a, 2012b, 2014).

6. Methodology

6.1. Field survey

The topographic surveying of the current shoreline and a geomorphological mapping of landforms found in the western part of the island of Naxos were conducted using DGPS-RTK (DGPS-Differential Global Positioning System-Real Time Kinematic) Spectra Precision SP80 GNSS Receiver.

6.2. GIS software

In the present study, the ArcGIS 10.4 program, and the ArcGIS Pro version 2.8 of ESRI (Environmental Systems Research Institute) has been used. The ArcGIS environment offers a number of applications, through the use of which maps with the digitized areas of interest were created, as well as the calculation of the CVI. Another ArcGIS tool used to calculate the seasonal shoreline shift for the individual shores of the study, but also for the coastal zone of Naxos, is DSAS 4.3 (Digital Shoreline Analysis System).

6.3. Coastal Vulnerability Index (CVI)

Various methods have been proposed and used from time to time to assess coastal erosion vulnerability based on a number of parameters such as coastal geomorphology, sea level rise, coastline evolution, etc., directly related to forthcoming climate changes and how they will impact sea level. One of the most common methods is the Coastal Vulnerability Index (CVI), introduced by Gornitz *et al*. (1990). It is a relatively simple and functional method of assessing the vulnerability to erosion of any coastal environment in relation to future sea level rise. It combines the sensitivity of the coastal zone to changes, with its ability to adapt to new conditions. By quantifying/calibrating the coastal zone vulnerability, we identify the areas that are comparatively more vulnerable to sea level change.

The vulnerability quantification, as originally proposed by Gornitz *et al*. (1990) (Table 3) for the east coast of America, was based on the interaction of seven variables. These variables are the topographical relief, the geology, the geomorphology, the vertical movements due to eustachianism or tectonic movements, the shoreline change, the tidal range, and the significant wave height. The qualitative and quantitative information incorporated in each variable receives values ranging from 1 to 5, with 5 representing the most vulnerable category of each variable.

CVI variables according to Gornitz *et al*. (1990)					
CVI	**Very Low**	**Low**	**Moderate**	**High**	**Very High**
Variables	1	2	3	4	5
Relief (m)	≥30.1	20.1-30.0	10.1-20.0	5.1-10.0	0-5.0
Geology	Plutonic, Volcanic, High-medium grade metamorphics	Low grade metamorphicsS andstones and Conglomerates	Most sedimentary rocks	Coarse and poorly sorted unconsolid-ated sediments	Fine unconsolid-ated sediments, Volcanic ash
Geomorphology	Rocky, Cliffed coasts, Fiords, Fiards	Medium Cliffs, Indented coasts	Low Cliffs, Glacial drift, Salt marsh, Coral reefs, Mangrove	Beaches (Pebbles), Estuary, Laggoon, Alluvial Plains	Barrier beaches (sand), Mudflats, Deltas
Vertical Movement (mm/yr)	≤-1.1	-1.0 to 0.99	1.0 to 2.0	2.1 to 4.0	≥4.1

Shoreline Displacement (m/yr)	≥2.1 Accretion	1.0 to 2.0	-1.0 to 1.0 Stable	-1.1 to -2.0	≤-2.0 Erosion
Tidal Range (m)	≤0.99 Microtidal	1.0 to 1.9	2.0 to 4.0 Mesotidal	4.1 to 6.0	≥6.1 Macrotidal
Wave Height Max (m)	0 to 2.9	3.0 to 4.9	5.0 to 5.9	6.0 to 6.9	≥7.0

Table 3: CVI variables according to Gornitz et al. (1990).

CVI was later modified (Gornitz *et al*., 1994) (Table 4) to include seven natural terrestrial/marine variables and six climate variables. The index was then further modified to arrive at its most common applicable form. In previous relevant studies (Gornitz *et al*., 1990; Shaw *et al*., 1998) beaches characterized by high tide/macro-tidal- (tidal range> 4 m) were ranked with high vulnerability, while micro-tidal shores (tidal range <2 m) were ranked as low vulnerability. This categorization was based on the notion that large tidal ranges are associated with strong tidal streams that affect coastal behavior. Thieler and Hammer Klose (1999), for estimating coastal vulnerability off the east coast of the Americas, chose to reverse this ranking so that long tidal coasts are characterized by low vulnerability.

CVI variables according to Gornitz *et al*. (1994)					
CVI	**Very Low**	**Low**	**Moderate**	**High**	**Very High**
Variables	1	2	3	4	5
Elevation	≥30.0	20.1-30.0	10.1-20.0	5.1-10.0	0-5.0
Geology	Plutonic, Volcanic, High-medium grade metamorphics	Low grade metamorphics Sandstones and Conglomerates	Most sedimentary rocks	Coarse, poorly sorted unconsolid-ated sediments	Fine unconsolid-ated sediments, Volcanic ash
Geomorphology	Rocky, Cliffed coasts, Fiords, Fiards	Medium Cliffs, Indented coasts	Low Cliifs, Glacial drift, Alluvial Plains	Cobble beaches, Estuary, Lagoon	Barrier beaches, Sand beaches, Salt marsh, Mud flats, Deltas, Mangrove, Coral reefs
RSL Change (mm/yr)	<-1.0	-1.0 to 0.9	1.0 to 2.0	2.1 to 4.0	>4.0

Mean Shoreline Displacement (m/yr)	>2.0 Accretion	1.1 to 2.0	-1.0 to +1.0	-1.1 to -2.0	<-2.0 Erosion
Mean Tide Range (m)	<1.0	1.0 to 1.9	2.0 to 4.0	4.1 to 6.0	>6.0
Maximum Significant Wave Height (m)	0.0 to 2.9	3.0 to 4.9	5.0 to 5.9	6.0 to 6.9	>6.9
Annual Tropical Storm prob. (%)	0.0 to 8.0	8.1 to 12.0	12.1 to 16.0	16.1 to 20.0	>20.0
Annual Hurricane prob. (%)	0.0 to 4.0	4.1 to 8.0	8.1 to 12.0	12.1 to 16.0	>16.0
Hurricane Frequency Intensity Index (%)	0.0 to 20.0	21.0 to 40.0	41.0 to 80.0	81.0 to 120.0	>121.0

Mean Forward Velocity (m/sec)	>15.0	15.0 to 12.0	12.1 to 9.0	9.1 to 6.0	<6.0
Annual Mean no. Extra-Tropical	0.0 to 10.0	10.1 to 20.0	20.1 to 30.0	30.1 to 40.0	>40.1
Mean Hurricane	0.0 to 2.0	2.1 to 4.0	4.1 to 6.0	6.1 to 7.0	>7.0

Table 4: CVI variables according to Gornitz et al. (1994).

This reasoning is mainly based on the possible effect of storms on coastal evolution in relation to the range of the tide. For example, on a tidal shoreline, there is only a 50% probability that a storm will occur during high tide. Therefore, for an area with a tide range of 4.0 m, a storm with a wave height of 3.0 m is still 1 m below the maximum tidal altitude for half a tidal cycle. On the other hand, a micro- tide coastline is virtually always "close" to high tide and therefore always runs a high risk of flooding from storms.

The CVI proposed by Thieler and Hammer Klose (1999) (Table 5) is similar to that used by Gornitz *et al*. (1994), as well as to the index used by Shaw *et al*. (1998). This indicator allows the connection of six natural variables in a quantifiable way. This method yields numerical figures that cannot be directly emulated to specific physical effects. However, it points out areas where the various effects of sea level rise may be larger. The Coastal Vulnerability Index has been widely used in applications and studies of different scales. In the literature there are various applications of CVI with modifications and incorporations of physical parameters for the adaptation of the index to the respective coastal study area (Abuodha *et al*., 2007; Srinivasa-Kumar *et al*., 2010; Pantusa *et al*., 2018).

CVI variables according to Thieler & Hammar -Klose (1999)					
CVI	**Very Low**	**Low**	**Moderate**	**High**	**Very High**
Variables	1	2	3	4	5
Geomorphology	Rocky, Cliffed coasts, Fiords, Fiards, Artificial Constructions	Medium Cliffs, Indented coasts	Low Cliffs, Glacial drift, Alluvial Plains, Beachrocks, Dunes, Mixed material	Cobble beaches, Estuary, Lagoon	Barrier beaches, Sand beaches, Salt marsh, Mud flats, Deltas, Mangrove, Coral reefs
Coastal Slope (%)	>11.5	11.5 to 5.5	5.5 to 3.5	3.5 to 2.2	<2.2
Relative Sea Level Change (mm/yr)	<1.8	1.8 to 2.5	2.5 to 3.0	3.0 to 3.4	>3.4
Shoreline Erosion/ Accretion (m/yr)	>2.0	1.0 to 2.0	-1.0 to +1.0	-1.1 to -2.0	<-2.0
Mean Tide Range(m)	>6.0	4.1 to 6.0	2.0 to 4.0	1.0 to 1.9	<1.0

Mean Wave Height (m)	<0.55	0.55 to 0.85	0.85 to 1.05	1.05 to 1.25	>1.25

Table 5: CVI variables according to Thieler & Hammar -Klose (1999).

Once the vulnerability value for each part of the coastline has been determined, based on the data of each variable, the CVI is calculated as the square root of the geometric mean or the square root of the product of the ranked variables divided by the total number of variables (i.e. six):

$$CVI = \sqrt{\frac{a * b * c * d * e * f}{6}}$$

where a = geomorphology, b = coastal slope, c = relative sea level change, d = shoreline erosion/accretion, e = mean tidal range and f = mean wave height.

6.4. CVI variables

6.4.1. Geomorphology

Coastal landforms can be identified from topographic diagrams, in which coastal landforms are often mentioned by name, such as sand, cliffs, coastal vegetation elements, etc. But mainly the information about the captured spatial entities such as swamps, lagoons, salt marshes, estuaries, are immediately usable, which leads directly to the determination of local geomorphology. Altitude information in the form of contour lines or individual altitudes, which provide information for local uplifts, steep coastal slopes or smooth shores, is also usable.

The variable of geomorphology is a non-numerical variable that expresses the relative response of different types of coastal geomorphic features to rising sea levels and their different resistance to the phenomenon of coastal erosion (Pendleton *et al.*, 2005). The qualitative classification of the different types of coastal geomorphic elements that occur in the respective study area, allows their subsequent rating on a scale from 1 to 5, with the coastal rocky cliffs presenting a very low risk (1), while the sandy shores present a particularly high risk (5) (Rao *et al.*, 2008; Karymbalis *et al.*, 2012).

For the assessment of coastal geomorphology, high, medium, and low slope cliffs, rocky shores, sandy beaches, beachrocks, lagoons, dune fields and anthropogenic structures were digitized in the environment of ArcGIS Pro version 2.8 software. A topographic map at the scale of 1:5,000, equidistant size 4.0 m was used, by the Hellenic Military Geographical Service – HMGS, of the year 1985.

6.4.2. Coastal Slope

The coastal slope is a geological variable directly related to the topography of an area. The identification of the coastal slope is used to determine the relative vulnerability of a coastal area to possible sea flooding and shoreline retreat, as low-altitude coastal areas with gentle slopes show greater vulnerability than steeper slopes (Pendleton *et al*., 2005; Karymbalis *et al*., 2012). For the calculation of the coastal slope (as a percentage) of the study area, a Digital Elevation Model (DEM) was created using detailed 4.0 m isometric curves and altitude points from 1:5,000 topographic diagrams by the Hellenic Military Geographical Service – HMGS. The slope was calculated for the whole island.

6.4.3. Relative Sea Level Change (RSL)

The relative sea level change variable results from an increase or decrease in the average annual water level, as measured by active tidal power stations (Pendleton *et al*., 2005). This variable concerns the global change of sea level mainly due to thermal expansion of the oceans and climate change. Specifically, according to the recent IPCC 2019 report, the RCP 2.6 scenario represents low greenhouse gas emissions and a high mitigation future, which in the CMIP5 simulations gives probability two out of three to limit global warming below 2 °C by 2100. This scenario predicts an increase in GMSL for the next 100 years to 0.43 m at a rate of 4.3 mm/year.

6.4.4. Shoreline Erosion/Accretion

The mean shoreline displacement variable refers to the shoreline displacement over time, determining the vulnerability of coastal areas and their response to shoreline retreat or accretion (Pendleton *et al*., 2010). Through the study of data such as orthophotos, maps and topographic diagrams, it is possible to compare the current state of the coastline with the form it had in previous years. In this way the shoreline shift trend is predicted, which trend is key information for understanding coastal processes and future changes (EUROSION, 2004; Mohanty *et al*., 2017). To determine the

displacement rate of the coastline of Naxos, compared to nowadays, topographic maps for the period 1985 were used. The digitization of the two coastlines was implemented in the ArcGIS Pro version 2.8 environment and the coastline displacement rate was calculated with the tool DSAS 4.3.

6.4.5. Mean Tidal Range

Tidal range is associated with permanent and episodic flood risks (Pendleton *et al*., 2005). The mean tidal range for a given tidal measuring station is defined as the difference in meters between the mean high tide and the mean low tide during a year. Considering the available statistics of the Hellenic Hydrographic Service from a tideographer in Syros, the mean tidal range is 14.0 cm.

6.4.6. Mean Wave Height

The significant wave height expresses the average of 1/3 of the highest waves of the total wave spectrum. Wave height is used as an indicator of wave energy, which increases the volume of coastal sediments. The wave heights that appear in the area, according to the Wind and Wave Atlas of the Hellenic Seas (Soukissian *et al*., 2007) of the Hellenic Center for Marine Research- HCMR, are 0.7-0.8 m.

6.5. DSAS

The DSAS tool is a software that allows the statistical calculation of the shoreline displacement rate (retreat/accretion) using historical shorelines in the form of vector data (Thieler *et al*., 2009). To calculate shoreline displacement, DSAS produces transects along the shoreline and perpendicular to a baseline. The distance between them and their length is determined by the user. The reference line is parallel to the historical coastlines and can be located either to the land or to the sea.

At the points where the transect lines intersect with the historic coastlines, points are generated that determine the locations of the historic shoreline locations along each transect. The statistical data are calculated for each transects line and are stored in a data table. Each method used to calculate the shoreline displacement rate is based on the measured differences between shoreline locations over time. The resulting values are expressed as measures of displacement of the shoreline position along the intersection lines per year (Himmelstoss, 2009). Negative values indicate a retreat of the coastline, while positive values indicate an accretion of the coastline.

The statistical method used through the DSAS 4.3 tool was NSM (Net Shoreline Movement). This method refers to the total distance between the older and newer coastline. The DSAS tool was also used to calculate the rate of displacement of the Naxos coastline, in the context of the implementation of the CVI, between the period 1985-2019. The statistical method used was EPR (End Point Rate). This method represents the distance of the coastlines for the time elapsed between the oldest and the newest coastline. Along the coastal zone of the study area, 2,163 cross-sectional lines were created at intervals of 20.0 m with from the reference line to the sea.

7. Coastal Vulnerability Index (CVI) calculation

The data were collected during the field work and topographic diagrams on a scale of 1:5,000 by the Hellenic Military Geographical Service – HMGS. The Hellenic Geodetic Reference System 1987 (EGSA 87-GreekGrid) was selected for the processing of the data and their imprint on maps in the ArcGIS 10.4 and ArcGIS Pro version 2.8 environment.

For each variable, the coast was categorized into five vulnerability categories, (1) very low, (2) low, (3) moderate, (4) high and (5) very high. Coastal rating limits into five risk categories have been proposed by Pendelon *et al*. (2004) (Table 6). The limits proposed by Alexandrakis *et al*., (2010) (Table 6) were used for the coastal slope variable.

CVI variables according to Pendleton *et al*. (2004)					
CVI	**Very Low**	**Low**	**Moderate**	**High**	**Very High**
Variables	1	2	3	4	5
Geomorphology	Rocky, Cliffed coasts, Fiords, Fiards, Artificial Constructions	Medium Cliffs, Indented coasts	Low Cliffs, Glacial drift, Alluvial Plains, Beachrocks, Dunes	Cobble beaches, Estuary, Lagoon	Barrier beaches, Sand beaches, Salt marsh, Mud flats, Deltas, Mangrove, Coral reefs
Coastal Slope (%) (Alexandrakis *et al*., 2010)	>12.0	12.0 to 9.0	9.0 to 6.0	6.0 to 3.0	<3.0

Relative Sea Level Change (mm/yr)	<1.8	1.8 to 2.5	2.5 to 3.0	3.0 to 3.4	>3.4
Shoreline Erosion/ Accretion (m/yr)	>2.0	1.0 to 2.0	-1.0 to +1.0	-1.1 to -2.0	<-2.0
Mean Tide Range (m)	>6.0	4.1 to 6.0	2.0 to 4.0	1.0 to 1.9	<1.0
Mean Wave Height (m)	<0.55	0.55 to 0.85	0.85 to 1.05	1.05 to 1.25	>1.25

Table 6: CVI variables according to Pendleton et al. (2004).

7.1. Geomorphology Variable

The main coastal landforms of the study area are the medium and low cliffs, rocky, cliffed coasts, intended coasts, cobble and sand beaches, lagoons, beachrocks and sand dunes as well. This category also includes artificial constructions such as the port of Naxos or smaller boat marinas which are marked by very low vulnerability. Most of the coastal zone of western Naxos (57.76%) (Table 7, Figure 15) consists of rocky cliffed coasts and artificial constructions and marked by very low vulnerability. The following percentage of the total length of the shoreline under study represents around 35.17% which is occupied by sand beaches and pocket beaches and is marked by very high vulnerability (Table 7, Figure 15). The 4.11% of the shoreline is occupied by cobble and pebble beaches, lagoons and beachrocks which are marked by high vulnerability (Table 7, Figure 15). Followed by 1.55% medium cliffs and intended coasts which are marked by low vulnerability, and with 1.41% low cliffs, beachrocks and dunes which are marked by moderate vulnerability (Table 7, Figure 15).

Vulnerability ranking	Very Low (1)	Low (2)	Moderate (3)	High (4)	Very High (5)	Total
Geomorphology	Artificial Constructions, Rocky Cliffed coasts	Medium Cliffs, Indented coasts	Low Cliffs, Beachrocks Dunes	Cobble, Pebble beaches, Lagoons	Sand beaches, Sandy Pocket beaches	
Length (%)	57.76	1.55	1.41	4.11	35.17	100.0
Length (km)	29.86	0.80	0.73	2.12	18.18	51.70

Table 7: Geomorphology variable ranking.

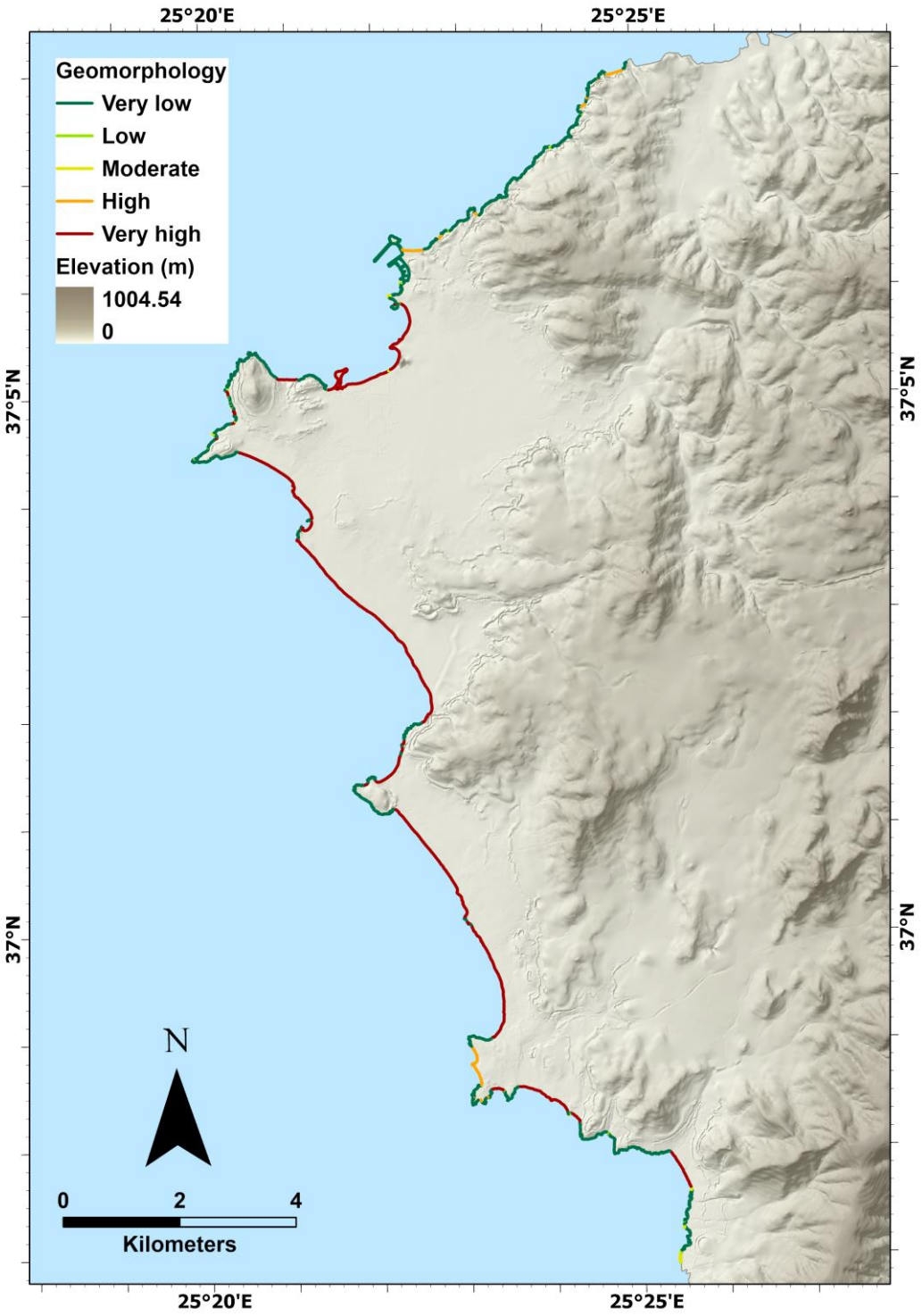

Figure 15: Map of vulnerability classification of the western Naxos coastline, according to the variable of Geomorphology.

7.2. Coastal Slope Variable

The coastal slope calculated for the distance between the shoreline and the contour line of 6m. In fact, 76.15% of the total length of the shoreline under study is marked by large slopes over 12.0% and, therefore, is characterized by very low vulnerability (Table 8, Figure 16).

An important point to consider is that in the western part of the island there are simultaneous parts of the shoreline with very low slopes (<3.0%) which are marked by very high vulnerability (Table 8, Figure 16). The remaining 4.70%, 4.04% and 2.32% correspond to high, moderate and low vulnerability respectively (Table 8, Figure 16).

Vulnerability ranking	Very Low (1)	Low (2)	Moderate (3)	High (4)	Very High (5)	Total
Coastal Slope (%)	>12.0	12.0 to 9.0	9.0 to 6.0	6.0 to 3.0	<3.0	
Length (%)	73.15	2.32	4.04	4.70	15.79	100.0
Length (km)	37.81	1.20	2.09	2.43	8.16	51.70

Table 8: Coastal slope variable ranking.

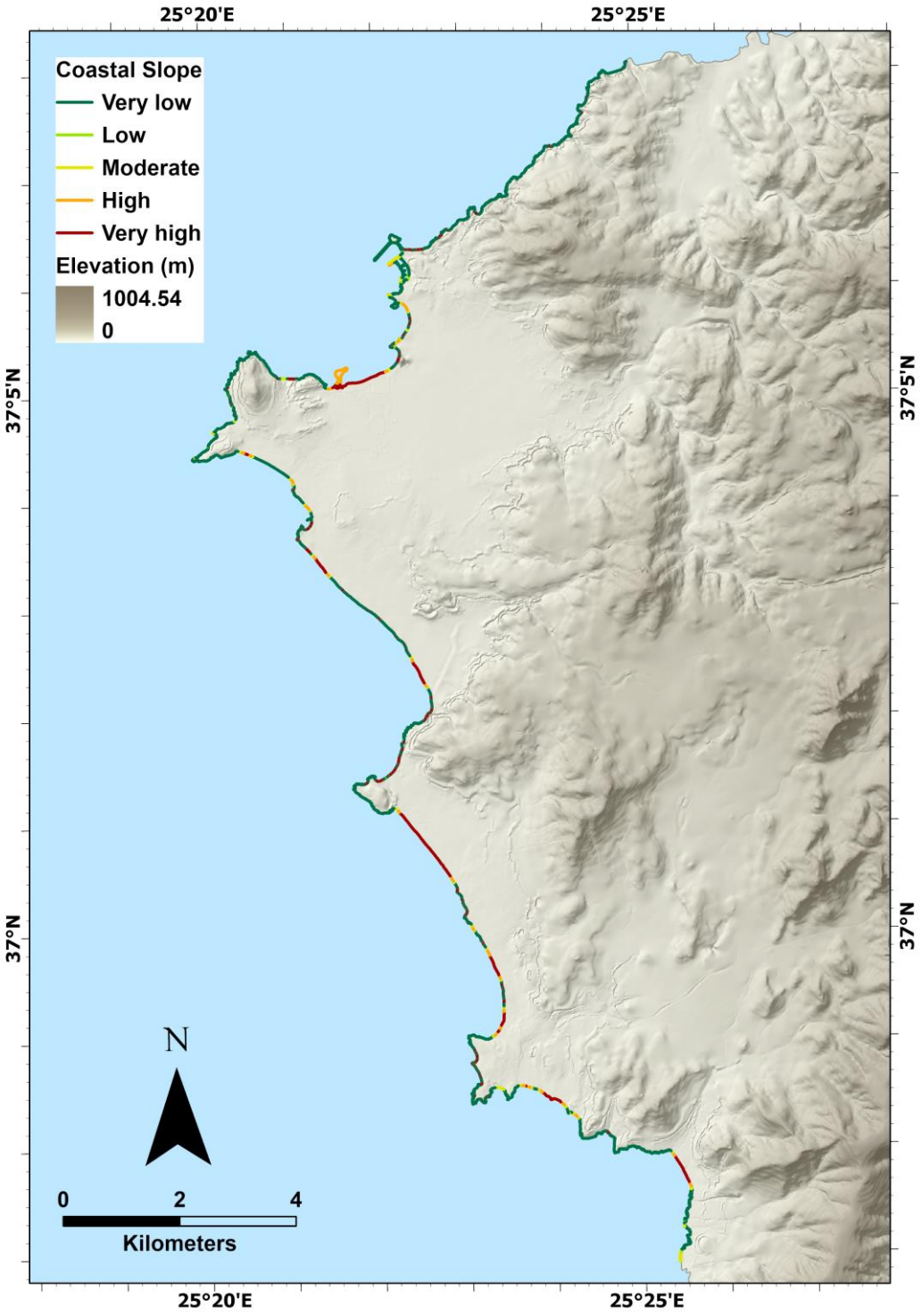

Figure 16: Map of vulnerability classification of the western Naxos coastline, according to the variable of coastal slope.

7.3. Relative Sea Level Change Variable

For the calibration of the relative sea level change, RCP 2.6 scenario of the IPCC 2019 report was applied, where for the next 100 years a rise of the sea level with a rate of 4.3 mm/yr is predicted (Table 9, Figure 17). The RCP 2.6 sea level rise scenario is characterized by very high vulnerability for the study area (Table 9, Figure 17).

Vulnerability ranking	Very Low (1)	Low (2)	Moderate (3)	High (4)	Very High (5)	Total
Relative Sea Level Change (mm/yr)	<1.8	1.8 to 2.5	2.5 to 3.0	3.0 to 3.4	>3.4	
Length (%)					100.0	100.0
Length (km)					51.70	51.70

Table 9: Relative Sea Level Change variable ranking.

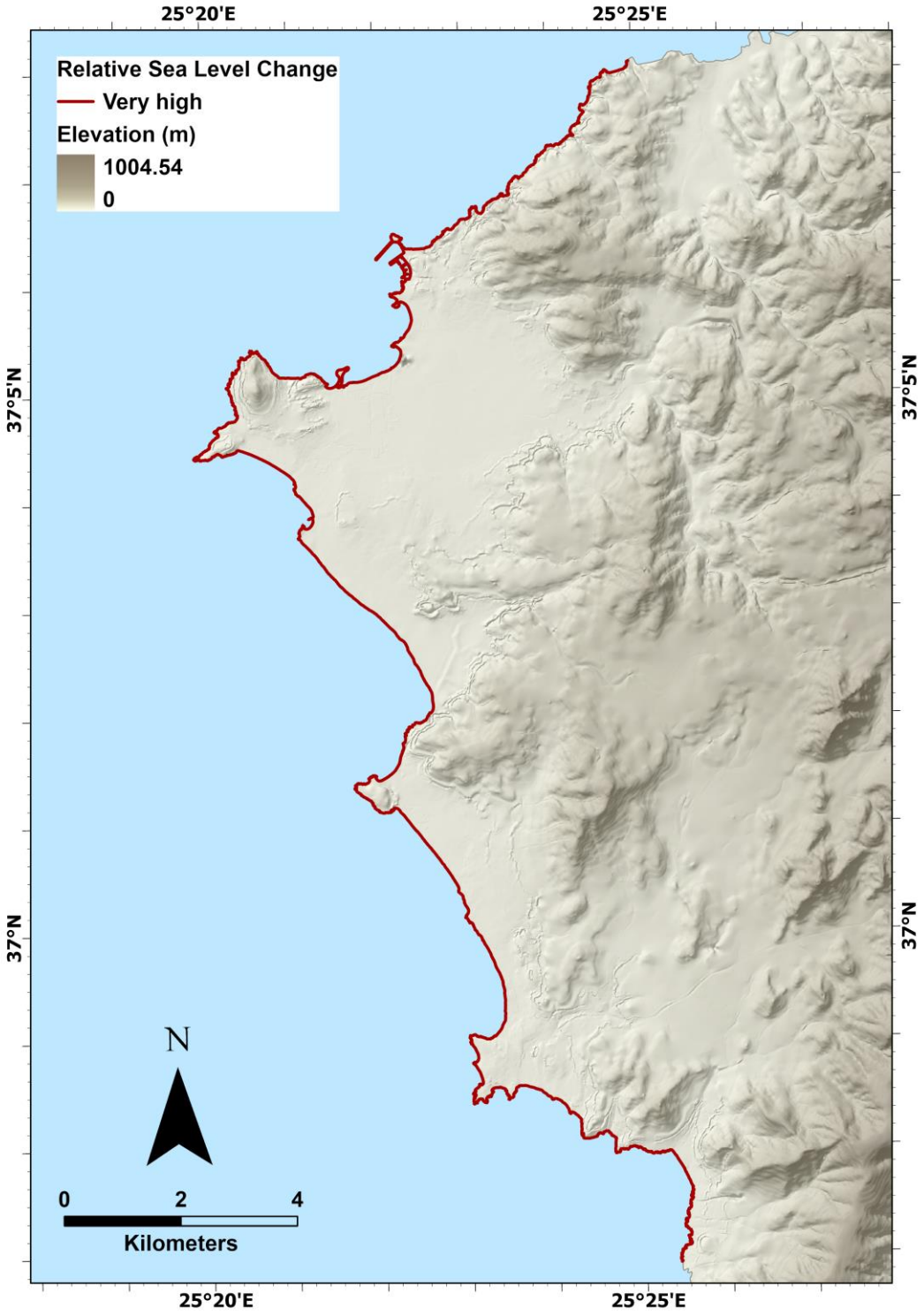

Figure 17: Map of vulnerability classification of the western Naxos coastline, according to the variable of Relative Sea Level Change.

7.4. Shoreline Erosion/Accretion Variable

The shoreline displacement rate was calculated using the DSAS 4.3 tool (Displacement rate= Distance/ (2019-1985)) based on digitized shorelines from the Hellenic Military Geographical Service – HMGS topographic diagrams, on a 1:5,000 scale, for the year 1985 and topographic surveying for the year 2019.

From the calculation of the displacement rate, it appears that most of the shoreline under study is marked by a rate of -0.16 to 0.18 m/yr (Table 10, Figure 18, 19). In order to calibrate the vulnerability, the ranges proposed in the list of references are taken into account. Therefore, the displacement rate for the entire shoreline under study for western Naxos falls into the category of moderate vulnerability.

Rate differentiation is only observed in Agios Georgios (Figure 18, 19). This area partially presents a different displacement rate integrating occasionally at very low vulnerability at a rate of 1.55 to 3.94 m/yr, low vulnerability at a rate of 0.18 to 1.55 m/yr, moderate vulnerability at a rate of -0.16 to 0.18 m/yr, high vulnerability at a rate of about -1.2 to -0.16 m/yr or very high vulnerability at a rate of -2.86 to -1.2 m/yr (Table 10, Figure 18, 19).

Vulnerability ranking	Very Low (1)	Low (2)	Moderate (3)	High (4)	Very High (5)	Total
Erosion/Accretion Rate (m/yr)	>2.0	1.0 to 2.0	-1.0 to 1.0	-2.0- to -1.0	<-2.0	
Length (%)	0.84	0.43	97.52	0.57	0.64	100.0
Length (km)	0.44	0.22	50.40	0.29	0.33	51.70

Table 10: Shoreline Erosion/Accretion variable ranking.

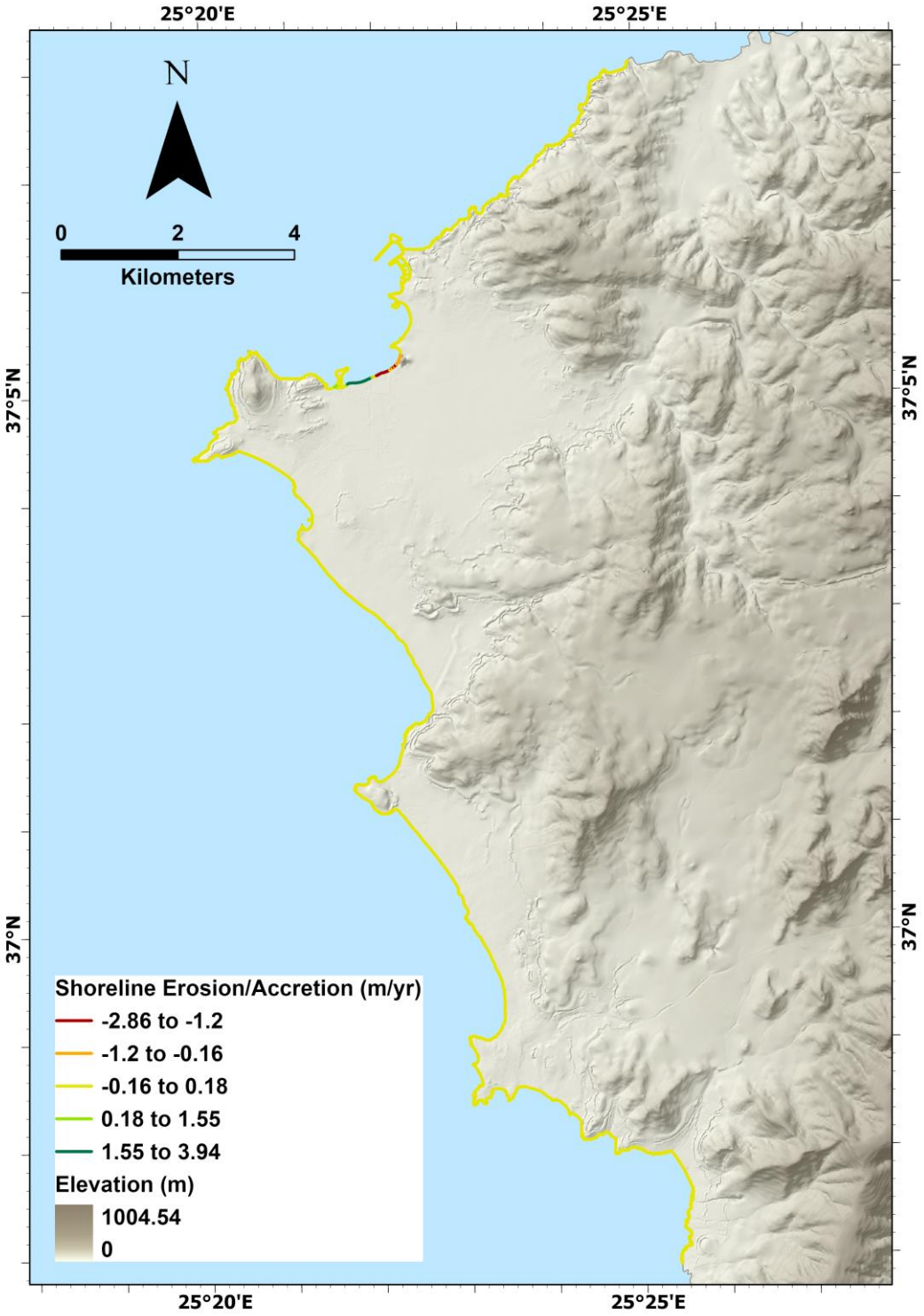

Figure 18: Map of vulnerability classification of the western Naxos coastline, according to the variable of Shoreline Erosion/Accretion rates.

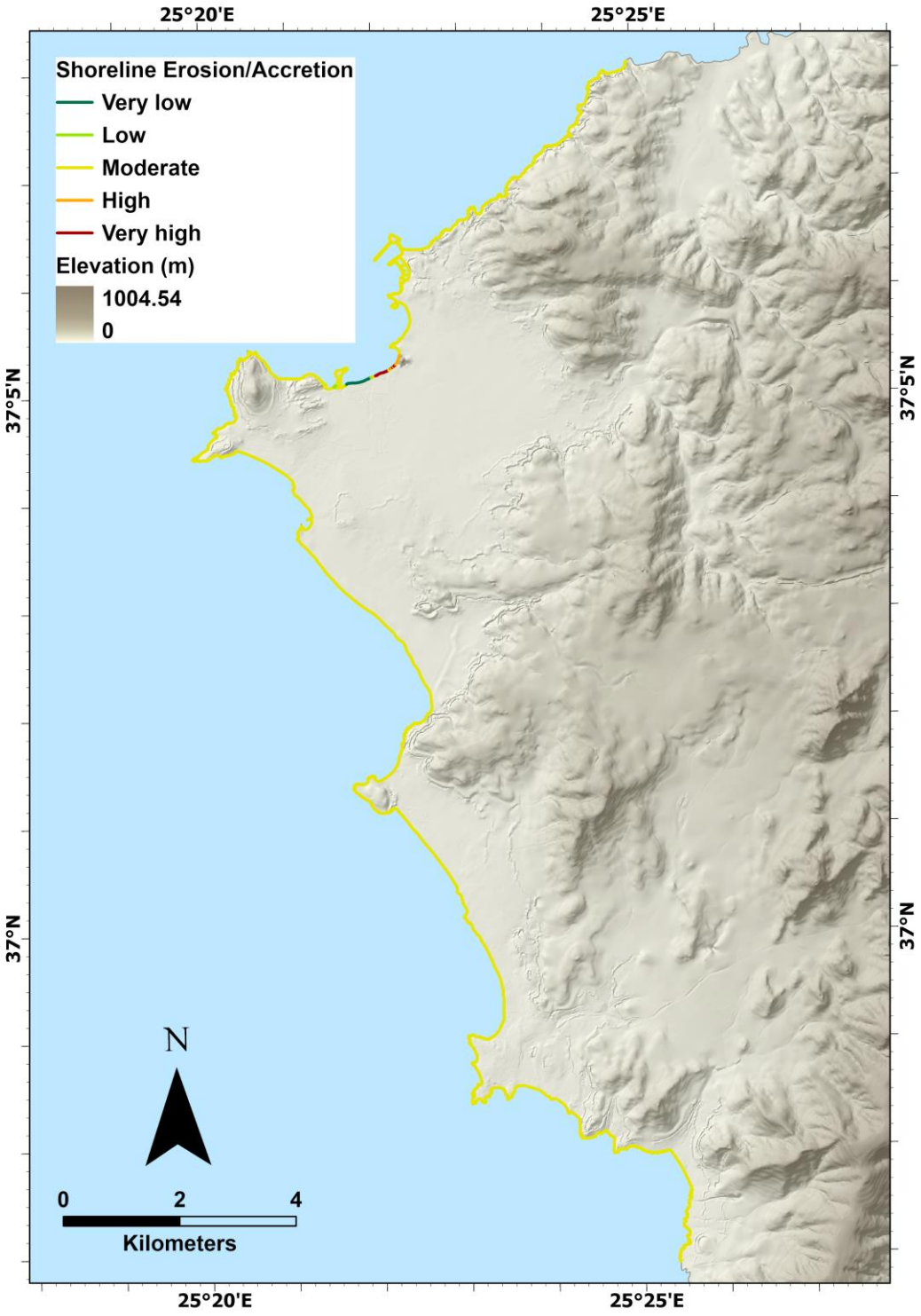

Figure 19: Map of vulnerability classification of the western Naxos coastline, according to the variable of Shoreline Erosion/Accretion.

7.5. Mean Tide Range Variable

Considering the available data of the Hellenic Hydrographic Service for the Cyclades complex, the mean tide range is 14.0 cm and was considered the same along the entire shoreline under study. Therefore, the entire shoreline of western Naxos falls into the category of very high vulnerability based on the references (Table 11, Figure 20).

Vulnerability ranking	Very Low (1)	Low (2)	Moderate (3)	High (4)	Very High (5)	Total
Mean Tide Range (m)	>6.0	4.0 to 6.0	2.0 to 4.0	1.0 to 2.0	<1.0	
Length (%)					100.0	100.0
Length (km)					51.70	51.70

Table 11: Mean Tide Range variable ranking.

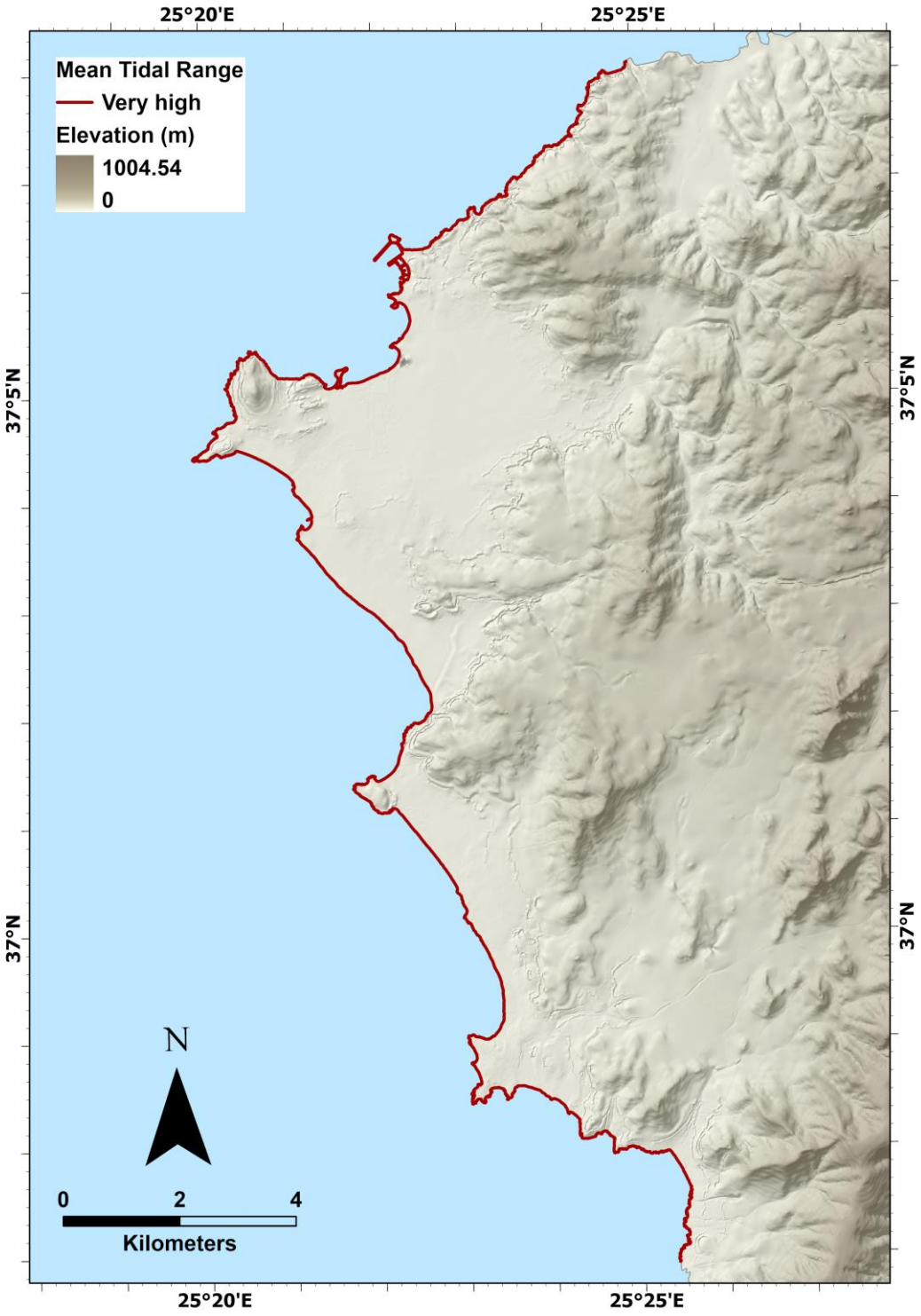

Figure 20: Map of vulnerability classification of the western Naxos coastline, according to the variable of Mean Tide Range.

7.6. Mean Wave Hight Variable

According to the Wave and Wind Atlas of the Hellenic Seas (Soukissian *et al.*, 2007) of the Hellenic Centre for Marine Research, the mean wave height variable for the study area is 0.7 to 0.8 m. Therefore, the entire shoreline under study in western Naxos falls into the category of low vulnerability (Table 12, Figure 21).

Vulnerability ranking	Very Low (1)	Low (2)	Moderate (3)	High (4)	Very High (5)	Total
Mean Wave Hight (m)	<0.55	0.55 to 0.85	0.85 to 1.05	1.05 to 1.25	>1.25	
Length (%)		100.0				100.0
Length (km)		51.70				51.70

Table 12: Mean Wave Hight variable ranking.

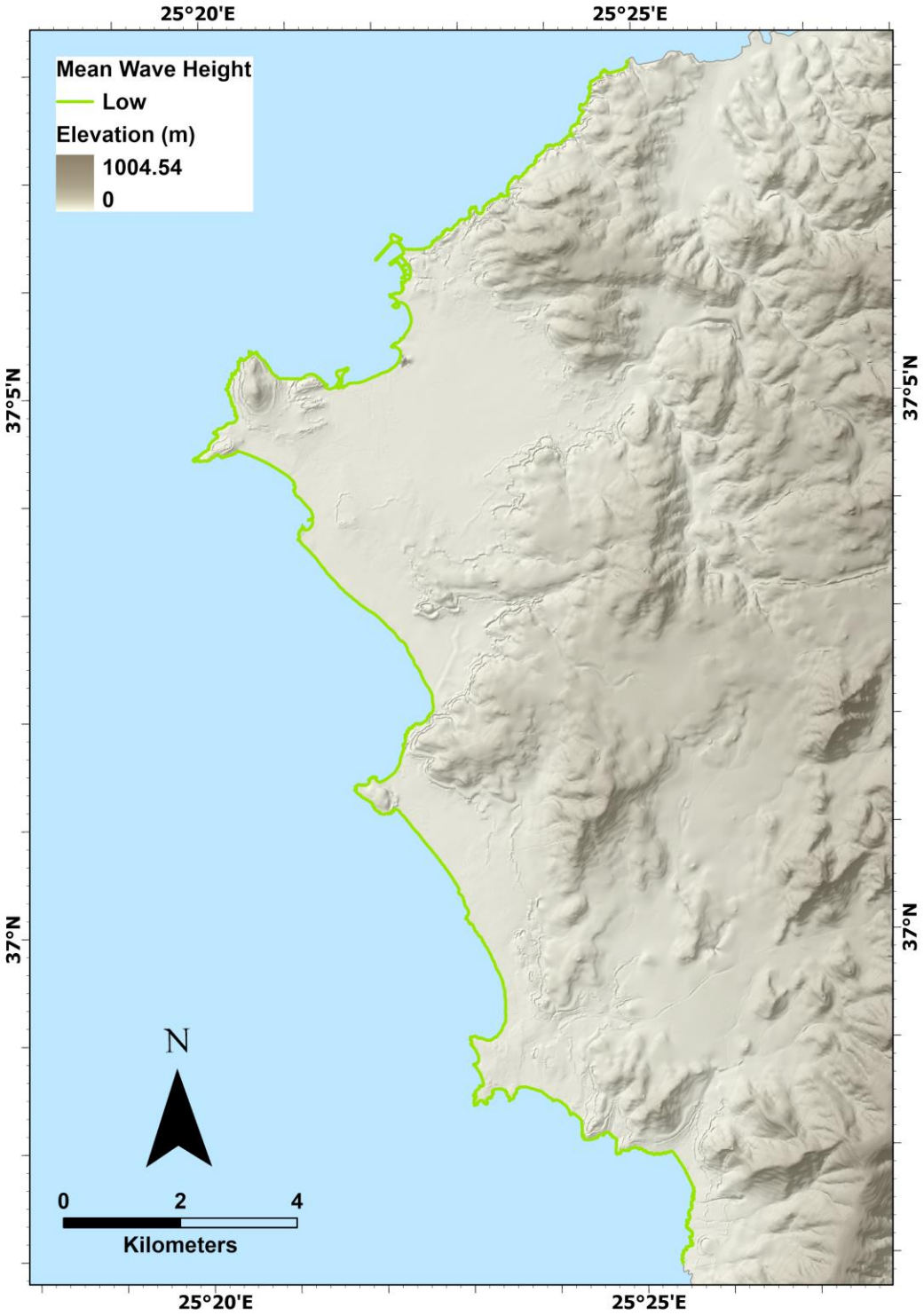

Figure 21: Map of vulnerability classification of the western Naxos coastline, according to the variable of Mean Wave Hight.

7.7. CVI Calculation

After calibrating the vulnerability of geological and natural variables to coastal erosion in relation to a future sea level rise, the mathematical calculation of the Coastal Vulnerability Inditex followed. Estimated CVI values along the shoreline under study range from 5.0 to 32.0 (Table 13, Figure 22).

Considering the 56.84% of the total length of the shoreline under study which corresponds to 29.39 km is characterized by very low vulnerability (Table 13, Figure 22). Followed by 18.48% of the total length of the shoreline under study which corresponds to 9.55 km and is characterized by low vulnerability. 12.80% of the total length of the shoreline under study which corresponds to 6.62 km and is characterized by very high vulnerability. 8.03% of the total length of the coastline under study which corresponds to 4.15 km and is characterized by high vulnerability (Table 13, Figure 22). The smallest percentage of the total shoreline under study is characterized by moderate vulnerability and corresponds to 3.83% (1.98 km) (Table 13, Figure 22).

Vulnerability ranking	Very Low (1)	Low (2)	Moderate (3)	High (4)	Very High (5)	Total
CVI	5.0 to 7.07	7.07 to 13.0	13.0 to 18.0	18.0 to 22.4	22.4 to 32.0	
Length (%)	56.84	18.48	3.83	8.03	12.80	100.0
Length (km)	29.39	9.55	1.98	4.15	6.62	51.70

Table 13: CVI variable ranking.

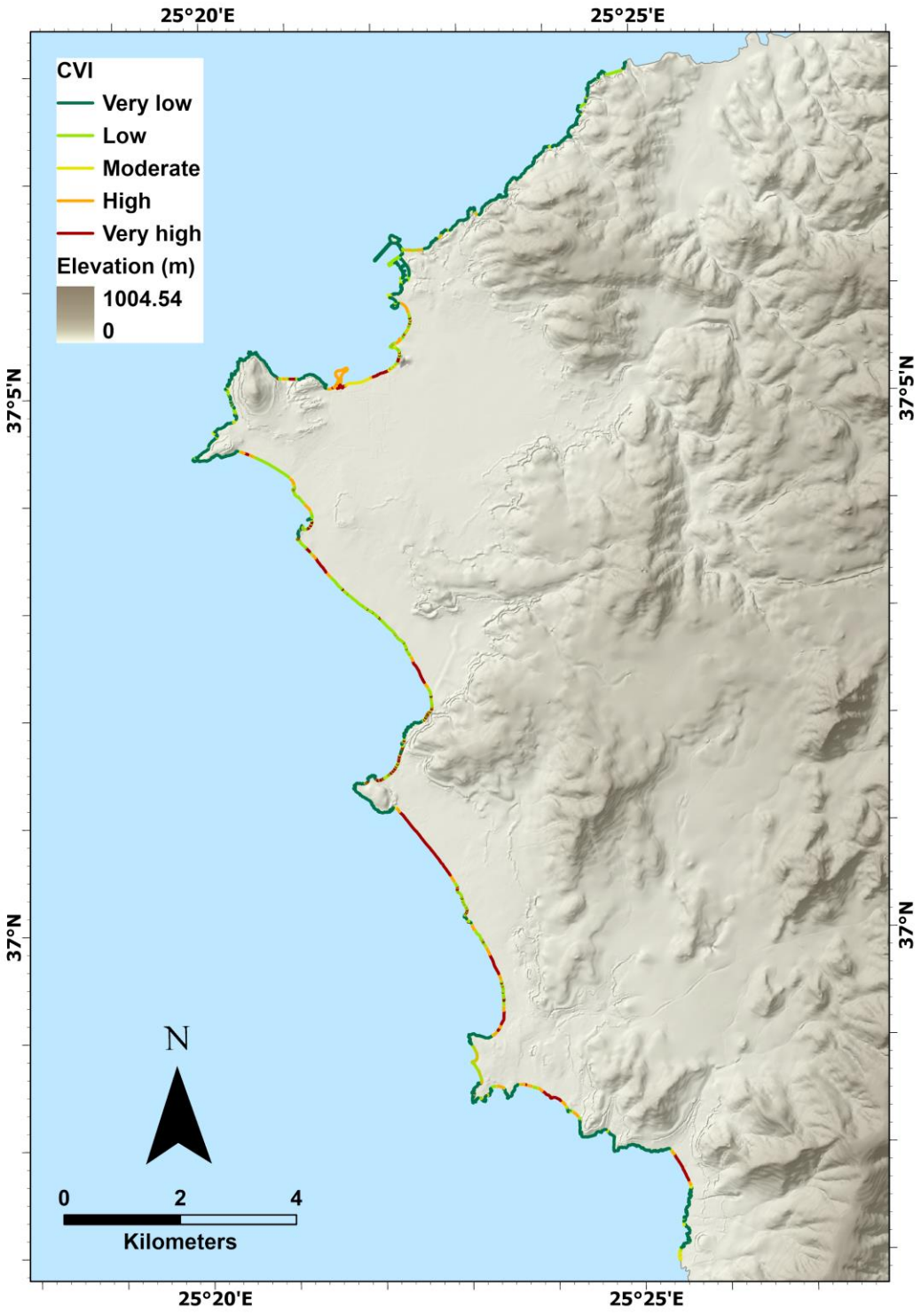

Figure 22: Coastal Vulnerability Index (CVI) map of the study area. The coastline is divided into five ranges (from very low to very high).

8. Results

In this study, the relative vulnerability of the coastal zone of western Naxos, in relation to a future sea level rise according to the IPCC 2019 scenarios, it was estimated by calculating the Coastal Vulnerability Index. After the geological and natural variables were calibrated, CVI values were calculated along the shoreline ranging from 5.0 to 32.0. Examining the overall vulnerability of the coastal zone of western Naxos, it is clear that among the five calibration categories, the vulnerability distribution is uneven with the very low vulnerability to outweigh.

The western coastal zone is composed of a sandy beach, bordered by low lying sand dunes, lagoons and an alluvial plain. These systems are becoming increasingly vulnerable, due to natural processes such as wave energy, but also due to human interventions that have significantly eliminated sediment input to the coastal zone and the increasing touristic development.

The geomorphology, as a non-numerical variable, expresses the relative response of different types of coastal landforms to sea level rise. It is ranked qualitatively according to the relative resistance of coastal landforms and rocks to erosion. The main coastal landforms at the study area (from very high to very low vulnerability) are sandy to gravelly beaches, developed especially where the main channels of the drainage networks meet the sea, pocket beaches, sand dunes, beachrocks, medium and low cliffs, indented coasts and rocky cliffed coasts.

Cliffs represent the dominant landform along the study area occupying a total length of 27.31 km, which corresponds to 52.82% of the total shoreline, followed by beaches (sand and cobble) with a total length of 21.07 km which is 40.75% of the total shoreline.

Lithological formations range in terms of their erodibility from non-cohesive sediments to hard rocks. About 41.90% of the coast is underlain by alluvial deposits, 9.10% is underlain by Neogene (marls) deposits, 38.40% is underlain by granodiorite deposits and 10.60% is underlain by marble and schists.

Among the considered variables, coastal slope and geomorphology are the main indicators of erodibility risk. The determination of regional coastal slope identifies the relative vulnerability and the potential rapidity of shoreline retreat. Coastal regions with

Low sloping should retreat faster than steeper ones. Regions with coastal slopes lower than 3.0% were characterized as of very high vulnerability, while coastal cliffs with slopes higher than 12.0% were of very low vulnerability.

A large percentage (56.84%) of the western coast is of low vulnerability area due to the presence of steep rocky cliffs. Agios Georgios, Agios Prokopios, Agia Anna, Plaka, Mikri Vigla, Kastraki, Pirgaki and Agiassos are the only low lying, classified as high and very high vulnerable areas of the western coast.

Relative sea-level change is considered to have the same value along the study area. Due to recent sea-level measurements, this variable took the value of 4.3 mm/yr (very high vulnerability), which is the mean eustatic global sea-level rise rate according RCP 2.6 scenario (IPCC, 2019).

Shorelines change rates in western part of Naxos Island incorporate from accretion equal to +0.18 m/yr (moderate vulnerability) to retreat equal to -0.16 m/yr (moderate vulnerability). Rate differentiation is only observed in Agios Georgios. This area partially presents a different displacement rate integrating occasionally between +1.55 to 3.94 m/yr or +0.18 to +1.55 m/yr or -1.2 to -0.16 m/yr or -2.86 to -1.2 m/yr. Approximately 50.40 km, which corresponds to 97.52% of the study's area coastline, is relatively stable, while 2.48% of the coastline is eroding (Agios Georgios area).

The western part of Naxos Island as part of the Aegean Sea is a microtidal region with tidal range <14.0 cm according to Hellenic Hydrographic Service for the Cyclades. As a result, the tidal variable is ranked with the value of very high vulnerability.

According to the Wave and Wind Atlas of the Hellenic Seas of the Hellenic Centre for Marine Research the mean wave height variable for the study area is 0.7 to 0.8 m. Wave heights are proportional to the square root of wave energy, which is a measure of the capacity for erosion. Western Naxos coastline length has been characterized of low vulnerability.

9. Conclusions

In this study the relative vulnerability of the western Naxos coast changes due to future rise of sea-level and estimated with the calculation of the Coastal Vulnerability Index (CVI). CVI values along the shoreline vary between 5.0 (very low vulnerability) and 32.0 (very high vulnerability). The vulnerability of the coast to sea-level rise is spatially non uniform because of variations in some of the incorporated variables. Thus, the variables introducing the greatest variability to the CVI values are those of geomorphology, shoreline accretion and/or erosion and regional coastal slope. Among the other three factors significant wave high, tidal range and relative sea-level change have the same values for the entire area.

According to the criteria of coastal vulnerability, as defined in this study, the sections of coast with the highest CVI ratings include low laying coasts, such as sandy beaches and pocket beaches. These highly vulnerable regions are the coastal areas of Agios Georgios, Agios Prokopios, Agia Anna, Plaka, Mikri Vigla, Kastraki, Pirgaki and Agiassos. Very low and moderate vulnerability is represented by steepy rocky coast areas.

10. References

1. Abuodha, P.A., Woodroffe, C.D., 2007. Assessing Vulnerability of Coasts to Climate Change: A Review of Approaches and Their Application to the Australian Coast; Australian National Centre for Ocean Resources and Security. University of Wollongong: Wollongong, Australia, 2007, 458p, Available online: http://citeseerx.ist.psu.edu/viewdoc/download?doi=10.1.1.461.2048&rep=rep1&type=pdf
2. Alexandrakis G., Karditsa A., Poulos S., Ghionis G., Kampanis N.A., 2010. An assessment of the vulnerability to erosion of the coastal zone due to a potential rise of sea level: The case of the Hellenic Aegean coast. In Environmental Systems – Volume III, [Ed. Achim Sydow], In: Encyclopedia of Life Support Systems (EOLSS), Developed under the Auspices of the UNESCO, Eolss Publishers, Oxford, UK, 324 p.
3. Altherr, R., Kreuzer, H., Wendt, I., Lenz, H., Wendt, I., Harre, W., Dürr, S., 1994. Further evidence for a late Cretaceous low pressure high temperature terrane in the Cyclades, Greece. Chemie der Erde, 54, 319–328.
4. Altherr, R., Schliestedt, M., Okrusch, M., Seidel, E., Kreuzer, H., Harre, W., Lenz, H., Wendt, I., Wagner, G.A., 1979. Geochronology of high-pressure rocks on Sifnos (Cyclades, Greece). Contributions to Mineralogy and Petrology, 70(3), 245-255.
5. Andriessen, P.A.M., Boelrijk, N., Hebera, E., Priem, H., Vermurden, E., Vershure, R., 1979. Dating the events of Metamorphism and granitic magmatism in the Alpine Oregon of Naxos (Cyclades Greece). Contributions to Mineralogy and Petrology 69, 215-225.
6. Avigad, D., Garfunkel, Z., 1989. “Low-Angle Faults above and below a Blueschist Belt?Tinos Island, Cyclades, Greece.” Terra Nova 1(2), 182–87.
7. Avigad, D., Garfunkel, Z., Jolivet, L., Azañón, J.M., 1997. “Back Arc Extension and Denudation of Mediterranean Eclogites.” Tectonics 16(6), 924–41.
8. Bernier, P., Guidi, J.B., Bottcher, M.E., 1997. Coastal progradation and very early diagenesis of ulramafic sands as a result of rubble discharge from asbestos excavations (northern Corsica, western Mediterranean). Marine Geology, 144, 163–175.

9. Blake, M.C., Bonneau, M., Geyssant, J., Kienast, J.R., Lepvrier, C., Maluski, H., Papanikolaou, D., 1981. A geological reconnaissance of the Cycladic blueschist belt, Greece. Geological Society of America Bulletin 92, 247– 254, doi:10.1130/0016-7606(1981)92<247:AGROTC>2.0 .CO;2.
10. Bonneau, M. 1982. "Evolution Geodynamique de l'arc Egeen Depuis Le Jurassique Superieur Jusqu'au Miocene." Bulletin de La Société Géologique de France S7-XXIV(2), 229–42.
11. Briguglio, L., 2004. Small Island Developing States and their Economic Vulnerabilities. International Workshop on 'Vulnerability and Resilience of Small States'. The Global Development Research Center Programme, Partner of UN Ocean Atlas, The Ocean Project, GIN Global Island Network, World Ocean Network, University Gozo Centre, Malta.
12. Buick, I.S., 1991, Mylonitic fabric development on Naxos: Journal of Structural Geology, v. 13, p. 643–655, doi:10.1016/0191-8141(91)90027-G.
13. Church, J.A., Clark, P.U., Cazenave, A., Gregory, J.M., Jevrejeva, S., Levermann, A.,Merrifield, M.A., Milne, G.A., Nerem, R.S., Nunn, P.D., Payne, A.J., Pfeffer, W.T., Stammer, D., Unnikrishnan, A.S., 2013. Sea-level rise by 2100. Science 342(6165), 1445-1445.
14. Church, J.A., White, N.J., 2011. Sea-level rise from the late 19th to the early 21st century. Surv. Geophys. 32(4–5), 585–602.
15. Church, J.A.,White, N.J., Konikow, L.F., Domingues, C.M., Cogley, J.G., Rignot, E., Gregory, J. M., van den Broeke, M.R., Monaghan, A.J., Velicogna, I., 2011. Revisiting the Earth's sea-level and energy budgets from 1961 to 2008. Geophys. Res. Lett. 38.
16. Collet, I., Engelbert, A., 2013. Coastal regions: people living along the coastline, integration of NUTS 2010 and latest population grid. EUROSTAT Stat. Focus, 30, 12.
17. Dangendorf, S., Hay, C., Calafat, F.M., Marcos, M., Piecuch, C.G., Berk, K., Jensen, J., 2019. Persistent acceleration in global sea-level rise since the 1960s. Nature Climate Change, 9(9), 705-710.
18. Davenport, J., Davenport, J.L., 2006. The impact of tourism and personal leisure transport on coastal environments: a review. Estuar. Coast. Shelf Sci. 67, 280–292.

19. Durr, S., 1986. Das Attisch-kykladische Kristallin, -116-167. In: Jacobshagen, V (Hrsg), Geologie von Griechenland, Beitrage zur Regionalen Geologie der Erde 19, p. 363. Gebr. Borntaeger, Berlin.
20. Durr, S., Flugel, E., 1979. Obertrias Fossilien in den Marmoren von Naxos, XXVIe Congres, Assemblee plenierem Monaco a Atalya/Tyrquie.
21. EUROSION, 2004. Living with coastal erosion in Europe: Sediment and Space for Sustainability. PART I - Major findings and Policy Recommendations of the EUROSION project. 57 (Directorate General Environment, European Commission).
22. Evelpidou, N., 2001. Geomorphological and Environmental study of Naxos island using Remote Sensing and GIS techniques. Phd Thesis in Greek, Faculty of Geology and Geoenvironment, National and Kapodistrian University of Athens. GAIA, 13, 226 p.
23. Evelpidou, N., Pavlopoulos, K., Vassilopoulos, A., Triantaphyllou, M., Vouvalidis, K., Syrides, G., 2012a. Holocene palaeogeographical reconstruction of the western part of Naxos island (Greece)», Quaternary International, 266, 81–93. doi: 10.1016/j.quaint.2011.08.002.
24. Evelpidou, N. Melini, D., Pirazzoli, P., Vassilopoulos, A., 2012b. « Evidence of a recent rapid subsidence in the S–E Cyclades (Greece): An effect of the 1956 Amorgos earthquake?», Continental Shelf Research, 39–40, 27–40. doi: 10.1016/j.csr.2012.03.011.
25. Evelpidou, N. Melini, D., Pirazzoli, P.A., Vassilopoulos, A., 2014. «Evidence of repeated late Holocene rapid subsidence in the SE Cyclades (Greece) deduced from submerged notches», International Journal of Earth Sciences, 103(1), 381–395. doi: 10.1007/s00531-013-0942-0.
26. Evelpidou, N., Pirazzoli, P., 2014. Holocene relative sea-level changes from submerged tidal notches: A methodological approach. Quaternaire 25(4), 383-390.
27. Evelpidou, N., Vassilatos, C., Anastasatou, M., Karkani, A. & Stamatakis, M., 2021. Factors controlling granitic cavernous weathering forms in a Mediterranean island: the case of Naxos island, Aegean Sea, Greece. Zeitschrift für Geomorphologie.
28. Feenstra, A., 1985. Metamorphism of Bauxites on Naxos, Greece, Geol, Ultraiectina, Vol. 39, p. 206, Utrecht.

29. Gautier, P., Brun, J.P., Jolivet, L., 1993. Structure and kinematics of Upper Cenozoic extensional detachment on Naxos and Paros (Cyclades Islands, Greece): Tectonics, v. 12, p. 1180–1194, doi:10.1029/93TC01131.
30. Ginsburg, R.N., 1953. Beachrock in south Florida. Journal of Sedimentary Petrology, 23: 85–92.
31. Gornitz, V., White, T.W., Cushman, R.M., 1990. Vulnerability of the East coast, U.S.A. to future sea level rise. J. Coast. Res., 9, 201–237.
32. Gornitz, V.M., Daniels, R.C., White, T.W. & K.R. Birdwell, 1994. The development of a coastal vulnerability assessment database, Vulnerability to sea-level rise in the U.S. southeast. Journal of Coastal Research, Special Issue No. 12, 327-338.
33. Goudie, A., Viles, H.A., 1997. Salt weathering hazard. Wiley.
34. Goudie, A.S., Viles, H.A., Parker, A.G., 1997. Monitoring of rapid salt weathering in the central Namib Desert using limestone blocks. Journal of Arid Environments, 37(4), 581-598.
35. Hallegatte, S., Green, C., Nicholls, R.J., Corfee-Morlot, J., 2013. Future flood losses in major coastal cities. Nat. Clim. Chang. 3(9), 802–806.
36. Hanor, J.S., 1978. Precipitation of beachrock cements: mixing of marine and meteoric waters vs. CO2-degassing. Journal of Sedimentary Petrology, 48: 489–501.
37. Himmelstoss, E.A., 2009. “DSAS 4.0 Installation Instructions and User Guide” in: Thieler, E.R., Himmelstoss, E.A., Zichichi, J.L., and Ergul, Ayhan. 2009 Digital Shoreline Analysis System (DSAS) version 4.0 — An ArcGIS extension for calculating shoreline change: U.S. Geological Survey Open-File Report 2008-1278.
38. Hinkel, J., Brown, S., Exner, L., Nicholls, R.J., Vafeidis, A.T., Kebede, A.S., 2012. Sea-level rise impacts on Africa and the effects of mitigation and adaptation: an application of DIVA. Reg. Environ. Chang. 12 (1), 207–224.
39. Huet, O., Dupic, L., Harrois, A., Duranteau, J., 2011. “Oxidative Stress and Endothelial Dysfunction during Sepsis.” Frontiers in Bioscience 16(5),1986–95.
40. IPCC, 2019. Summary for Policymakers. In: IPCC Special Report on the Ocean and Cryosphere in a Changing Climate [H.O. Pörtner, D.C. Roberts, V. Masson-Delmotte, P. Zhai, M. Tignor, E. Poloczanska, K. Mintenbeck, M. Nicolai, A. Okem, J. Petzold, B. Rama, N. Weyer (eds.)]. In press.

41. Jansen J., 1977. The geology of Naxos. Institute of Geological and Mining Research, Greece.
42. Jansen, J.B.H., Schuilimg, R.D., 1976. Metamorphism on Naxos: petrology and geothermal gradients. American Journal of Science, 276(10), 1225-1253.
43. Jolivet, L., Brun, J.P., 2010. Cenozoic geodynamic evolution of the Aegean. Interna1178 tional Journal of Earth Sciences, 99(1), 109–138. doi: 10.1007/s00531-008-0366-4.
44. Karkani, A., 2017. Study of the geomorphological and environmental evolution of the coastal zone of Central Cyclades. Phd thesis. Faculty of Geology and Geoenvironment, National and Kapodistrian University of Athens.
45. Karkani, A., Evelpidou, N., Vacchi, M., Morhange, C., Tsukamoto, S., Frechen, M., Maroukian, H., 2017. Tracking shoreline evolution in central Cyclades (Greece) using beachrocks. Marine Geology, 388, 25-37.
46. Karymbalis, E., Chalkias, C., Chalkias, G., Grigoropoulou, E., Manthos, G., Ferentinou, M., 2012. Assessment of the sensitivity of the southern coast of the Gulf of Corinth (Peloponnese, Greece) to sea-level rise. Central European Journal of Geosciences, 4(4), 561-577.
47. Kemp, A.C., Horton, B.P., Donnelly, J.P., Mann, M.E., Vermeer, M., Rahmstorf, S., 2011. Climate related sea-level variations over the past two millennia. Proc. Natl. Acad. Sci. U. S. A. 108(27), 11017–11022.
48. Kober, L., 1928. Der Bau der Erde: eine Einführung in die Geotektonik. Gebr. Bornträger.
49. Krumbein, W.E., 1979. Photolithotropic and chemoorganotrophic activity of bacteria and algae as related to beachrock formation and degradation (Gulf of Aqaba, Sinai). Geomicrobiology, 1, 139–203.
50. Lister, G.S., Davis, G.A., 1989. The origin of metamorphic core complexes and detachment faults formed during Tertiary continental extension in the northern Colorado River region, U.S.: Journal of Structural Geology.
51. Mellor, A., Short, J., Kirkby, S.J., 1997. Tafoni in the El Chorro area, Andalucia, southern Spain. Earth Surface Processes and Landforms: The Journal of the British Geomorphological Group, 22(9), 817-833.
52. Mentaschi, L., Vousdoukas, M. I., Pekel, J.-F., Voukouvalas, E., Feyen, L., 2018. Global long-term observations of coastal erosion and accretion. Sci. Rep. 8, 12876.

53. Milne, G.A., Gehrels, W.R., Hughes, C.W., Tamisiea, M.E., 2009. Identifying the causes of sea-level change. Nat. Geosci. 2(7).
54. Mimura, N., 2013. Sea-level rise caused by climate change and its implications for society. Proc. Jpn. Acad. Ser. B Phys. Biol. Sci. 89(7), 281–301.
55. Mohanty, P.C., Mahendra, R.S., Nayak, R.K., Kumar, T.S., 2017. Impact of sea level rise and coastal slope on shoreline change along the Indian coast. Natural Hazards, 89(3), 1227-1238.
56. Molenaar, N., Venmans, A.A.M., 1993. Calcium carbonate cementation of sand: a method for producing artificially cemented samples for geotechnical testing and a comparison with natural cementation processes. Engineering Geology, 35, 103–122.
57. Oppenheimer, M., Glavovic, B.C., Hinkel, J., van de Wal, R., Magnan, A.K., Abd-Elgawad, A., Cai, R., Cifuentes-Jara, M., DeConto, R.M., Ghosh, T., Hay, J., Isla, F., Marzeion, B., Meyssignac, B., Sebesvari, Z., 2019. Sea Level Rise and Implications for Low-Lying Islands, Coasts and Communities. In: IPCC Special Report on the Ocean and Cryosphere in a Changing Climate [H.-O. Pörtner, D.C. Roberts, V. Masson-Delmotte, P. Zhai, M. Tignor, E. Poloczanska, K. Mintenbeck, A. Alegría, M. Nicolai, A. Okem, J. Petzold, B. Rama, N.M. Weyer (eds.)]. In press.
58. Pantusa, D., D'Alessandro, F., Principato, F., Tomasicchio, G.R., 2018. Application of a Coastal Vulnerability Index. A Case Study along the Apulian Coastline, Italy. Water — Open Access Journal. Water 2018, 10, 1218; doi:10.3390/w10091218
59. Pendleton, E.A., Thieler, E.R., Williams, S.J., 2005. Coastal Vulnerability Assessment of War in the Pacific National Historical Park to Sea-Level Rise. U.S. Geological Survey Open-File Report 2005a-1056. 2005. Available online: https://pubs.usgs.gov/of/2005/1056/.
60. Pendleton, E.A., Thieler, E.R., Williams, S.J., 2010. Importance of coastal change variables in determining vulnerability to sea-and lake-level change. Journal of Coastal Research, 176-183.
61. Pirazzoli, P.A. 1986. Marine notches. In Sea-level research (pp. 361-400). Springer, Dordrecht.
62. Poulos, S.E., Chronis, G., 1997. The importance of the river systems in the evolution of the Greek coastline. Bulletin-Institut Oceanographique Monaco-Numero Special-, 75-96.

63. Rao, K.N., Subraelu, P., Rao, T.V., Malini, B.H., Ratheesh, R., Bhattacharya, S., Rajawat, A.S., 2008. Sea-level rise and coastal vulnerability: an assessment of Andhra Pradesh coast, India through remote sensing and GIS. Journal of Coastal Conservation, 12(4), 195-207.
64. Reinecke, T., Altherr, R., Hartung, B., Hatzipanagiotou, K., Kreuzer, H., Harre, W., 1982. Remnants of a Late Cretaceous hightemperature belt on the island of Anafi (Cyclades, Greece). Neues Jahrbuch fur Mineralogie, Abhandlungen, 145, 157–182.
65. Ring, U., Glodny, J., Will, T., Thomson, S., 2007. An Oligocene extrusion wedge of blueschist-facies nappes on Evia, Aegean Sea, Greece: implications for the early exhumation of high-pressure rocks. Journal of the Geological Society, 164(3), 637-652.
66. Ring, U., Glodny, J., Will, T., Thomson, S., 2010. The Hellenic subduction system: high-pressure metamorphism, exhumation, normal faulting, and large-scale extension. Annual Review of Earth and Planetary Sciences, 38(1), 45-76.
67. Schmalz, R.F., 1971. Formation of beach rock at Eniwetok Atoll. In Bricker, O.P., (ed.), Carbonate Cements. Baltimore: Johns Hopkins University Press, pp. 17–24.
68. Scoffin, T.P., Stoddart, D.R., 1987. Beachrock and intertidal cements. In Scoffin, T.P. (ed.), An Introduction to Carbonate Sediments and Rocks. Glasgow: Blackie Publishing Company, pp. 401–425.
69. Shaked, Y., Avigad, D., Garfunkel, Z., 2000. Alpine high-pressure metamorphism at the Almyropotamos window (southern Evia, Greece). Geological Magazine, 137(4), 367-380.
70. Shaw, J., Taylor, R.B., Forbes, D.L., Ruz, M.H., Solomon, S., 1998. Sensitivity of the Canadian Coast to Sea-Level Rise. Geological Survey of Canada Bulletin, 505, 114 p.
71. Soukissian, T., Hatzinaki, M., Korres, G., Papadopoulos, A., Kallos, G., Anadranistakis, E., 2007. Wave and wind Atlas of the Hellenic Seas, Hellenic Centre for Marine Research Publ.
72. Srinivasa-Kumar, T., Mahendra, R.S., Nayak, S., Radhakrishnan, K., Sahu, K.C., 2010. Coastal Vulnerability Assessment for Orissa State, East Coast of India. J. Coast. Res. 2010, 26, 523–534.
73. Stoddart, D.R., Cann, J.R., 1965. Nature and origin of beach rock. Journal of Sedimentary Petrology, 35(1), 243–273.

74. Strahler, A.N., 1957. Quantitative analysis of watershed geomorphology. American Geophysical Union Transactions, 38(6), 912-920.
75. Strasser, A., Davaud, E., and Jedoui, Y., 1989. Carbonate cements in Holocene beachrock: example from Bahiret el Biban, southeastern Tunisia. Sedimentary Geology, 62, 89–100.
76. Taylor, J.C.M., Illing, L.V., 1969. Holocene intertidal calcium carbonate cementation, Qatar, Persian Gulf. Sedimentology, 12, 69–107.
77. Theocharatos, G., 1978. The climate of Cyclades. PhD Thesis, University of Athens, Greece.
78. Thieler, E.R., Hammar-Klose, E.S., 1999. National Assessment of Coastal Vulnerability to Sea-Level Rise, U.S. Atlantic Coast. U.S. Geological Survey, Open-File Report, 99-593 pp.
79. Thieler, E.R., Himmelstoss, E.A., Zichichi, J.L., Ergul, A., 2009. The Digital Shoreline Analysis System (DSAS) version 4.0-an ArcGIS extension for calculating shoreline change (No. 2008-1278). US Geological Survey.
80. Thorstenson, D.C., Mackenzie, F.T., Ristvet, B.L., 1972. Experimental vadose and phreatic cementation of skeletal carbonate sand. Journal of Sedimentary Petrology, 42(1), 162–167.
81. van Hinsbergen, D.J.J., Zachariasse, W.J., Wortel, M.J.R., Meulenkamp, J.E., 2005. "Underthrusting and Exhumation: A Comparison between the External Hellenides and the 'Hot' Cycladic and 'Cold' South Aegean Core Complexes (Greece)." Tectonics 24(2):n/a-n/a.
82. Vanderhaeghe, O., 2004, Structural development of the Naxos migmatite dome, in Whitney, D.L., Teyssier, C., and Siddoway, C.S., eds., Gneiss Domes in Orogeny: Geological Society of America Special Paper 380, p. 211–227.
83. Vousdoukas, M.I., Ranasinghe, R., Mentaschi, L., Plomaritis, T. A., Athanasiou, P., Luijendijk, A., Feyen, L., 2020. Sandy coastlines under threat of erosion. Nature climate change, 10(3), 260-263.
84. Wijbrans, J.R., McDougall, I., 1986. "40Ar/39Ar Dating of White Micas from an Alpine High-Pressure Metamorphic Belt on Naxos (Greece): The Resetting of the Argon Isotopic System." Contributions to Mineralogy and Petrology 93(2), 187–94.

85. Wijbrans, J.R., McDougall, I., 1988. “Metamorphic Evolution of the Attic Cycladic Metamorphic Belt on Naxos (Cyclades, Greece) Utilizing 40Ar/39Ar Age Spectrum Measurements.” Journal of Metamorphic Geology 6(5), 571–94.
86. Wijbrans, J.R., Schliestedt, M., York, D., 1990. “Single Grain Argon Laser Probe Dating of Phengites from the Blueschist to Greenschist Transition on Sifnos (Cyclades, Greece).” Contributions to Mineralogy and Petrology 104(5), 582–93.
87. Zeffren, S., Avigad, D., Heimann, A., Gvirtzman, Z., 2005. Age resetting of hanging wall rocks above a low-angle detachment fault: Tinos Island (Aegean Sea): Tectonophysics, v. 400, p. 1–25, doi:10.1016/j.tecto.2005.01.003.